

1967

A pilot experimental investigation of A514 steel beam-columns

Noichiro Okuto
Lehigh University

Follow this and additional works at: <https://preserve.lehigh.edu/etd>



Part of the [Civil Engineering Commons](#)

Recommended Citation

Okuto, Noichiro, "A pilot experimental investigation of A514 steel beam-columns" (1967). *Theses and Dissertations*. 3545.
<https://preserve.lehigh.edu/etd/3545>

This Thesis is brought to you for free and open access by Lehigh Preserve. It has been accepted for inclusion in Theses and Dissertations by an authorized administrator of Lehigh Preserve. For more information, please contact preserve@lehigh.edu.

A PILOT EXPERIMENTAL INVESTIGATION
OF A514 STEEL BEAM-COLUMNS

by
Koichiro Okuto

A Thesis
Presented to the Graduate Faculty
of Lehigh University
in Candidacy for the Degree of
Master of Science

Lehigh University
1967

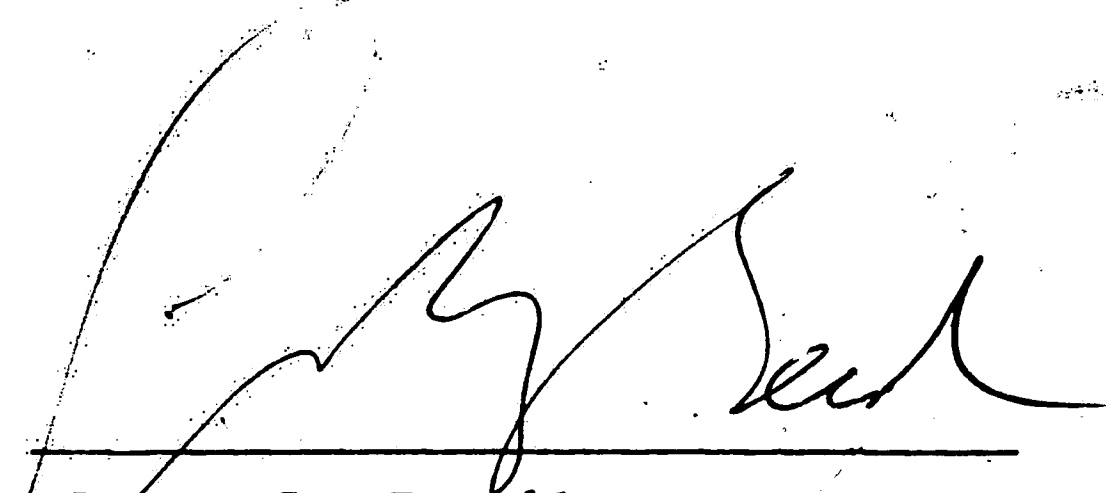
This thesis is accepted and
approved in partial fulfillment of
the requirements for the Degree of
Master of Science

May 22, 1967

Date



Lambert Tall
Professor in charge



Lynn S. Beedle
Acting-Chairman
Department of Civil Engineering

ACKNOWLEDGEMENTS

This thesis presents a pilot, experimental investigation into the strength of A514 steel beam-columns. The work is a part of an overall research project on "Welded Built-Up and Rolled Heat-Treated "T-1" Steel Columns" sponsored by the U. S. Steel Corporation, and conducted at the Fritz Engineering Laboratory, Civil Engineering Department, Lehigh University, Bethlehem, Pennsylvania. Lynn S. Beedle is acting-Chairman of the department and director of the Laboratory.

Acknowledgements are due to Charles G. Schilling of U. S. Steel Corporation and to John A. Gilligan, Chairman of Column Research Council Task Group 1 for their valuable guidance and comments. Special appreciation is due to Lambert Tall who supervised this thesis and who is the director of the project. Thanks are also due to the author's colleagues, especially to Ching K. Yu who assisted in various parts of the study.

ABSTRACT

A pilot experimental investigation was carried out on the behavior of A514 beam-columns. The test program included two beam-column tests, (one rolled heat-treated 8WF40 and one welded built-up 11" x 10-3/4" H-section,) and preliminary tests consisting of coupon tests, residual stress measurements and stub column tests.

The test procedures are presented in detail. Experimental results are compared with various exact and empirical theories used for predicting beam-column strength.

The test results indicated that A514 steel beam-columns had strengths higher than those of other steel mainly because of the higher yield point. They also check with the theoretical and empirical predictions currently used in design.

It is recognized that the rotation capacity of A514 beam-columns should be predicted by considering the effect of residual stresses, material properties and the strain reversal phenomenon.

TABLE OF CONTENTS

ACKNOWLEDGEMENT	Page
ABSTRACT	
I. INTRODUCTION	1
II. DESCRIPTION OF TESTS	3
1. Preliminary Tests	3
Tensile Coupon Tests	3
Residual Stress Measurements	6
Stub-Column Tests	8
2. Beam-Column Tests	9
Specimens	9
Apparatus	9
Measurement	10
Test Data	11
III. THEORETICAL ANALYSIS	14
1. Literature Review	14
2. Comparison of Obtained Data with Theories	16
3. Factors Affecting the Strength of T-1 Beam-Columns	18
IV. SUMMARY	20
V. TABLES AND FIGURES	23
VI. REFERENCES	53
VITA	

LIST OF TABLES

- Table 1 Chemical Composition and Minimum
 Mechanical Properties of "T-1" Steel
- Table 2 Mill Sheet Data
- Table 3 Summary of Tension Coupon Test Data

LIST OF FIGURES

- Fig. 1 Sections Investigated
- Fig. 2 Specimen Layout
- Fig. 3 Typical Coupon Test Data
- Fig. 4 Summarized Stress-Strain Relationship
- Fig. 5 Residual Stresses in 8WF40 Section
- Fig. 6 Residual Stresses in 11H66 Section
- Fig. 7 Typical Residual Stress Patterns
- Fig. 8 Stub Column Test for 8WF40 Section
- Fig. 9 Stub Column Test for 11H66 Section
- Fig. 10 General Layout of Specimen
- Fig. 11 Schematic Representation of Load Application
- Fig. 12 Mechanism of Lateral Bracing
- Fig. 13 Test Setup
- (a) General Test Setup
- (b) Jack Pressure Converter
- (c) End Rotation Gage
- Fig. 14 Instrument Layout
- Fig. 15 Behavior of 8WF40 Beam-Column
- Fig. 16 Behavior of 11H66 Beam-Column
- Fig. 17 Moment Deflection Curve, 8WF40 Beam-Column

- Fig. 18 Difference of the Moment Reading
- Fig. 19 — Local Buckling Behavior, 8WF40
- Fig. 20 Failure Mode, 8WF40 Beam-Column
- Fig. 21 . Failure Mode, 11H66 Beam-Column
- Fig. 22 Loading Conditions for Beam-Column
- Fig. 23 Test Data and Interaction Curves
- Fig. 24 End Moment-End Rotation Curve
- Fig. 25 Moment-Thrust-Curvature Curves

I. INTRODUCTION

Low-alloy high-strength constructional steel is one of the most attractive materials recently developed for steel structures. But, the somewhat different behavior from plain carbon structural steel requires several precautions in the application of this kind of steel. The use of high-strength steel is not yet included in the AISC specifications.

However, stimulated by their desirable characteristics, many structures are now designed and constructed of it, and several specifications and local codes are coming to recognize this fact. This paper deals with a study about the behavior of high-strength steel beam-columns.

Beam-columns are essential parts of almost every structure and most buildings have these parts as sub-assemblages. Thus their behavior is very necessary to be understood and so, there have been a number of research studies carried out to investigate them.

However, investigations concerning low-alloy high-strength constructional steels are not easily applicable especially when their plastic behavior is involved. Most design criteria are derived from extrapolation procedures based on the research of beam-columns made of low-carbon

steels; otherwise they are expressed as empirical formulas. There are problems in correlating this structural behavior to the basic properties of the members and materials. (1)

The present paper discusses a pilot experimental study with some theoretical considerations.

"T-1" steel is used in this investigation as the low-alloy high-strength steel. "T-1" steel is constructional alloy steel that meets the ASTM specifications A514 and/or A517. The common properties of this steel, as given by the fabricator, are shown in Table 1. (2),(3)

II. DESCRIPTION OF TESTS

In this series of pilot investigations, the following tests were carried out.

- a. Tensile coupon tests
- b. Residual stress measurements
- c. Stub column tests
- d. Beam-Column tests

Material was supplied by the U. S. Steel Corp., in four beams each 20' long; two were rolled 8WF40 and the other two were 11H66 flame-cut and welded sections.* Figure 1 shows the dimensions of each cross-section and Fig. 2 shows the portions used in the four tests above. Table 2 summarizes the millsheet that came together with this particular heat of material.

1. Preliminary Tests

Preliminary tests consisted of tensile coupon tests, residual stress measurements, and stub column tests.

Tensile Coupon Tests

A total of thirteen tensile coupon tests were carried out in the present series of tests. Coupons were prepared according to the ASTM specifications⁽⁴⁾ for test

* The identification, H, is used here to indicate a welded built-up wide flange section.

procedures, and their dimensions are tabulated in Table 3, together with the data obtained.

The purpose of executing these tests was to check if the properties of the present material are identical to those surveyed in the previous study, and if the static yield stress concept is applicable, especially at the knee of the stress-strain curve.

A specific procedure during testing was taken up to examine the latter purpose, that is, stopping the application of the load at several points right after attaining the elastic limit of this material. According to the concept which has been utilized to find the yield stress level, (5) the above-mentioned procedure should give the proper static relationship of stress and strain in the range between elastic limit and onset of strain hardening. One example of the data is shown on Fig. 3.

From this data, it was concluded that the present material is similar to that in the previous study.

For the study of the static behavior of structures and structural components, the static properties of materials have proved preferable. (5), (6) Several tests were carried out in the overall study in order to define them for "T-1" steel. (7) The data from those coupon tests are collected and summarized.

Statistical analyses can be applied for these sets of data. One representative stress-strain relationship is constructed by simple statistics and shown in Fig. 4. (8)

$$\frac{\sigma}{\sigma_y} = \sum_{i=0}^n c_{i1} \left(\frac{\epsilon}{\epsilon_y} - c_{i2} \right)^i \quad (1)$$

where

σ, ϵ : stress and strain variables

σ_y, ϵ_y : yield stress and yield strain

n, i, c_{i1}, c_{i2} : are constants

Figure 4 indicates the significant difference of this material compared to plain carbon mild steel.

- (1) A considerably curved knee between the elastic limit and the start of strain hardening part.
- (2) A very early occurring of strain hardening.
- (3) Almost no plateau of yield stress.

The conventional treatment of this kind of steel in the structural field, however, considers a bilinear elastic-perfect-plastic representation of stress and strain relationships. For the theoretical study in this paper, also, the bilinear relationship is used.

Residual Stress Measurements

Residual stresses in members are considered to be a factor which affects the beam-column's ultimate strength. Also, as for the pinned-end column's behavior, almost no satisfactory prediction can be made without considering residual stresses, especially for welded construction. (9)

Residual stresses are locked-in stresses in the structure induced by strain differences from neighboring portions of material. They are induced by several causes; that is, thermal stresses, phase transformations and so on, which in turn are caused by fabricating conditions, that is, heat-treatment, welding, cold working and others. Because of the many factors influencing the pattern and distribution of residual stresses, it is difficult to predict theoretically the residual stress in a section.

Residual stress effects on the structure, however, are caused mainly by the residual stresses that are oriented to the same direction as the applied load. The studies reported here are dependent on this fact, and were measured by the sectioning method. (6)

Residual stress measurements were carried out, one from each section. The results, magnitudes and distributions of residual stresses, are shown in Figs. 5 and 6,

for rolled 8WF40, and flame-cut and welded 11H66 sections respectively.

A small amount of tensile stress at the juncture of the flange and web of the rolled section, and a significant amount of tensile stresses at the tips of the flame-cut flange and the welded juncture of the flange to web of the welded sections are observed.

There have been reported several investigations concerning residual stress distributions of "T-1" steel sections. (7) They are summarized and schematically represented in Fig. 7. A typical residual stress pattern in mild steel sections is included also. Comparison can be made as follows:

(1) The magnitude of residual stress in terms of the yield stress, σ_r/σ_y , does not remain constant from one kind of steel to another.

(2) The maximum compression residual stresses in rolled sections are smaller in magnitude than those in welded built-up sections.

(3) It is clearly understood that the main causes of residual stress formation have significant effects on these distributions. They are

1. The difference of cooling rate in the rolled section, at the tips of flanges and

at the hot spots, at the juncture of a flange to the web.

2. Heat input by welding and flame-cutting.

(4) The measured residual stresses showed fairly symmetric patterns. This indicates that the cold working effect may not be so significant.

(5) The data shown in Figs. 5 and 6 are compared with the ones shown in Fig. 7 and are recognized not too different from them.

Stub Column Tests

Two stub column tests, one from each cross-section, were performed in order to obtain the average compressive stress-strain relationship for the complete cross-section. This relationship includes the effect of the residual stress. The length of stub columns should be sufficiently long to retain the original magnitude of residual stresses and short enough to prevent any premature failure from occurring before the yield load of the section is obtained. (9), (10) In this study the lengths

2' - 6" for rolled 8WF40 and

3' - 0" for welded 11H66 section

were used.

The average stress-strain curves obtained from the stub-column tests are given in Figs. 8 and 9. It is shown

from these curves, as expected, that the residual stresses lower the proportional limit according to their magnitudes.

2. Beam-Column Tests

Specimens

The general layout of the specimen is shown in Fig.10. The length of specimen controls the geometry. The slenderness ratio was decided first, then all other dimensions were determined consequently. A total length of 12' - 4" was used for the 8WF40 columns, and 16' - 8" was used for the 11H66 column. Other dimensions were designed also proportionally to each cross-sectional dimension.

Moment arms were designed to apply bending moments on both ends. The length was decided by the capacity of the jack which applied the bending force. E11018 low hydrogen electrodes were used for welding the connections and joints.

Apparatus (11)

The 5-million pounds tension-compression machine was used in order to apply the compressive force on the column because this machine has not only a sufficient capacity, but also is designed for the use of convenient test frames.

This compressive force was applied through the end fixtures and allowed free rotation at both ends. This means that these columns are both pinned-end columns. The schematic view of force application is shown in Fig. 11. The bending moments were applied by a hydraulic jack.

This type of beam-column will fail in one of three modes; bending, local buckling and lateral torsional buckling. (12) In order to prevent the latter failure, lateral bracing is used in practice. This problem was considered before conducting the test in the present investigation. Special lateral bracing, which was recently developed in the Fritz Laboratory, was used with very slight modification; modification of the width of clamping device in order to match the larger wide flange sections. The schematic view of this bracing is shown in Fig. 12. (13) It is composed of three bars and four spherical joints and allows only four possible movements of braced column. This suffices to fix the inplane behavior of the specimen. The location of the bracing is checked by the general design criteria. (14)

The pictures of the test setup are shown in Fig. 13.

Measurement

Figure 14 presents the general idea for the reading of data as well as the location of the lateral bracing. The 5-million pound machine itself gave the compressive

force applied to the column. The total axial compression force was maintained for these tests at 55% of the section's yield strength.

Bending moment was measured by three means. The hydraulic jack pressure indicated the force applied, the dynamometer, inserted in series with the jack, indicated the real force, and four sets of SR-4 strain gages were used to check the amount of applied moments at each end of the column.

Another set of strain gages, as well as these four sets, was also used to examine the real stress and strain distributions at representative sections.

Rotation levels on both ends of the column indicated the end rotations. Dial gages in two directions at mid-height indicated the in-plane and lateral deflections. Gage holes were drilled on both flanges at mid height of the column and measured to obtain the strains there, helping the check of deformations at the critical point. Micro-meter readings of the flange distance were taken at each increment of load. They furnished the local buckling behavior of two flanges.

Test Data

The overall behavior of specimens is shown in Fig. 15 and 16, with the prediction curves which correspond to the M- θ curves.

The theoretical prediction and the test data agree with each other generally.

8WF40 Shape

The failure mode was by local buckling which occurred at load number 22, that is, $\theta = 0.043$ and $M/M_{pc} = 0.44$. Maximum end moment attained was 118 ft-kips or $M/M_{pc} = 55.4\%$. The predicted value for $L/r = 37$ and $\sigma_y = 120$ ksi was 113 ft-kips or $M/M_{pc} = 53\%$, and the difference from the predicted value was four percent. However, on this prediction curve the clear length between two moment arms was used which gives an $L/r = 37$. This is simply to avoid the effect of the stiffness at joints which may affect the actual L/r .

11H66 Shape

The combination of the local buckling and the lateral torsional buckling occurred at about load number 21 after attainment of the ultimate moment leading to the complete failure of the 11H66 specimen. The observed maximum end moment was 250 ft-kips or $M/M_{pc} = 50.0\%$. The predicted value for the same L/r and σ_y value as before was 249 ft-kips or $M/M_{pc} = 49.8\%$, and the difference from the predicted value was negligible. Some other data obtained in these tests are shown, as example, in Fig. 17 through Fig. 19

Figure 17 shows the moment deflection curve for 8WF40 with the simple elastic theoretical line which agrees very well in the elastic portion of the behavior.

The comparison of the moment reading is shown on Fig. 18. The deviations referred to the dynamometer readings seem to be sufficiently small for both strain gage reading and jack pressure reading.

Mid-height local buckling behavior is summarized in Fig. 19 for the 8WF40 shape. In this figure, the thick lines on each flange indicate their horizontal movement referring to the scale shown on top. Pronounced local buckling was noticed at load number 22 for 8WF40, and at load number 21 for 11H66.

Figures 20 and 21 show the close up view of the failure mode for the sections 8WF40 and 11H66 respectively.

III. THEORETICAL ANALYSIS AND TEST RESULTS

1. Literature Review

The most fundamental consideration of column behavior with end moments is the one expressed in the elastic range.

$$EI \frac{d^2 v}{dz^2} + Pv + M = 0 \quad (2)$$

where

E: Modulus of Elasticity (Young's Modulus)

I: Moment of Inertia of cross-section

v: Deflection at z

z: Longitudinal location of cross-section

P: Compressive force

M: Equal end moment applied at both ends

for the case shown in Fig. 11.

The subassemblage cases considered in beam-column studies are divided into those shown in Fig. 22. For the case other than case "c" and "e", the M-term in Eq.(2) is linearly proportional to the variable, z. Equation (2) can be solved elastically in either case, the answers are given in several references. (15)

In the plastic range, however, because of the fact that the E and I terms are not constant, a direct explicit solution of Eq. (2) is not available conveniently. Consequently

numerical methods to approach the solution have been developed. Design data based on these numerical methods for the plain carbon steel are summarized in the references (16) and (17); but not directly applicable to the case of low-alloy high-strength structural steel.

Considering the variables E and I in the plastic range, Eq. (2) has to be broken into two primary static equilibrium equations

$$\int_A E_s y^2 \frac{d^2 v}{dz^2} dA + Pv + M = 0$$

(3)

$$\text{and } \int_A E_s y \frac{d^2 v}{dz^2} dA + P = 0$$

where

E_s : the ratio of stress to strain; in the elastic range $E_s = E$

y : distance of a fiber considered in a cross-section from the neutral axis

dA : cross-section area of a fiber considered

The numerical methods to solve this equation consist of two steps. The first is to establish the $M - P - \theta$ relationship using an appropriate E_s -value; the second is to calculate the $M - \theta$ curve using the $M - P - \theta$ relationship developed above. The E_s -value in Eq. (3) depends both upon material properties and upon the residual stress distribution.

All studies carried out in previous investigations (12), (18), (19) assumed a bilinear stress-strain relationship of plain carbon steel and measured or assumed residual stress distributions. In this study bilinear stress-strain characteristics were also assumed.

2. Comparison of Obtained Data with Theories

As stated before, there are several studies available on the strength of low-alloy, high-strength structural steel beam-columns. (9), (16) Formulas derived from these studies are also available, even though some are empirically determined and some are extrapolated from the data of plain carbon steel.

The test results obtained in the present study, two circles, are compared with two formulas, solid and dotted curves, in Fig. 23.

The solid curve in Fig. 23 presents the Massonnet equation, which is empirically derived as follows (9)

$$\frac{P}{P_u} + \frac{M_o}{M_u} \left(\frac{1}{1 - \frac{P}{P_e}} \right) = 1 \quad (4)$$

where

P = applied axial load

P_u = axial load producing failure in the
absence of bending moment

P_e = elastic critical load for buckling in the strong plane

M_o = Maximum applied moment, not including contribution of axial load interacting with deflections

M_u = Bending moment producing failure in the absence of axial load

The broken curve presents the analytical solution calculated by the extrapolation procedure, based on ASTM-A36 steel and extrapolating by the following.

$$\left(\frac{L}{r}\right)_{eq} = \left(\frac{L}{r}\right)_{\sigma_y} \times \sqrt{\frac{\sigma_y}{36}}, \quad \theta_{eq} = \theta_{\sigma_y} \times \sqrt{\frac{\sigma_y}{36}} \quad (5)$$

where

$\left(\frac{L}{r}\right)_{eq}, \left(\frac{L}{r}\right)_{\sigma_y}$: equivalent and actual slenderness ratios of high strength steel

$\theta_{eq}, \theta_{\sigma_y}$: equivalent and actual end rotations

σ_y : yield stress of high-strength steel in ksi.

It can be seen from Fig. 23 that the two empirical and extrapolation predictions are reasonably accurate, so that as far as the moment capacity of the beam-column is concerned, they can be recommended for the use in design.

3. Factors Affecting the Strength of "T-1" Beam-Columns

However, as Figs. 15 and 16 indicate, rotation capacities are not yet predicted well. The rotation capacity of the beam-column may be considered as a problem of plastic design and is discussed in several references. (14)

Figure 24 shows, for example, the calculated M- θ curves for the 11H66 section, the difference between the extrapolation procedure, which is described above, and the direct integration procedure, which is accomplished through two equilibrium equations, described in Eq. (3).

It is noticed in Fig. 24 that not only the maximum ultimate moments, but also the rotation capacities of this beam-column, differ by a fairly wide range.

The direct integration procedure curve is calculated using the idealized bilinear elastic-plastic relations of "T-1" steel and including the effect of residual stresses.

The M-P- θ relationship used in the direct integration procedure is compared with other M-P- θ curves in Fig. 25.

Because of the residual stress effect, the curve for the 11H66 sections deviates from the elastic line at an early stage of applied moment. This tends to reduce the maximum moment attained in the M- θ curve, but at the same time may increase the θ -values at which the maximum moment is attained.

The use of non-bilinear material properties, which have been shown in Fig. 4, may change this behavior also. This problem is yet to be determined.

Another aspect of the M- θ curves, Figs. 15 and 16, which should be considered, is the effect of the strain reversal. There are fairly wide discrepancies in these figures between theoretical predictions of the direct integration method and the test data, after the attainment of the ultimate moment.

The test data usually is difficult to obtain accurately, but commonly differ from the theoretical prediction. It should be noted that the theoretical prediction does not include the effect of strain reversal.

The effect of strain reversal is often considered in the problem of alternating plasticity and it is the influence of the unloading of portions which have gone into the plastified range. This effect is often neglected in design method, since it is believed that to go further would be impractical. (1)

However, in order to construct design procedures for higher strength steels, this should be another problem to be studied thoroughly.

IV. SUMMARY

This paper describes a pilot study of the strength of A514 steel beam-columns; "T-1" steel was used for this study.

A514 steel is becoming common in the field of building construction as a result of other uses in the structural field.

Basic preliminary tests, static coupon tests, residual stress measurements, and stub-column tests are carried out, studied, and compared with previous empirical investigations.

Two A514 beam-columns were tested and compared with theoretical predictions based on the results of a major research program at the Fritz Engineering Laboratory, Lehigh University, into the strength and behavior of rolled beam-columns of structural carbon steel.

The experiments included two wide flange beam-columns; one was a rolled and heat-treated 8WF40, the other a welded built-up 11H66 section.

The correlation between experimental results and various exact and empirical theories for beam-column strength is discussed. The main conclusions are as follows:

1. As far as the bending strength of beam-columns is concerned, the theoretical and empirical predictions currently used for the design of beam-columns made of structural carbon steel are applicable for the moment capacity of A514 beam-columns through the extrapolation procedure. (Fig. 23)
2. There are three main considerations which should be taken into account concerning the prediction of rotation capacities as well as the strength of A514 beam-columns: namely, the effect of residual stress, the effect of material property, and the effect of strain reversal.
3. The effect of residual stresses has been considered in the extrapolation procedures. The magnitude considered there is a typical pattern for A36 rolled sections. For A514 steel, as well as for other steels and fabrication procedures, different residual stress distributions have been observed. They play different roles on the beam-column behavior.
4. The material properties are represented by bilinear stress strain relationships. This idealization is applicable for mild steel. Although the same idealized curve was used in the theoretical prediction, it should be recognized further that A514 steel has somewhat different characteristics, and these may need further consideration.

5. The effect of strain reversal is considered as the possible explanation of the post-buckling behavior of an A514 beam-column under load. This was not included in the theoretical calculation, but should be studied thoroughly in order to establish completely the design procedures for the high-strength low-alloy constructional steels.

V. TABLES AND FIGURES

TABLE 1

CHEMICAL COMPOSITION AND MINIMUM
MECHANICAL PROPERTIES OF "T-1" STEEL

1. Chemical Composition

C	0.10-0.20	Ni	0.70-1.00
Mn	0.60-1.00	Cr	0.40-0.65
P	0.035 max	Mo	0.40-0.60
S	0.040 max	V	0.03-0.08
S _i	0.15-0.35	Cu	0.15-0.50
		B	0.002-0.006

2. Mechanical Properties

Yield Strength

Ext. Under Load

100,000 psi

Tensile Strength

115,000-140,000 psi

Elongation in 2 in., min.

18%

Reduction of Area, min.

45%

TABLE 2 MILL SHEET DATA

1. Chemical Composition

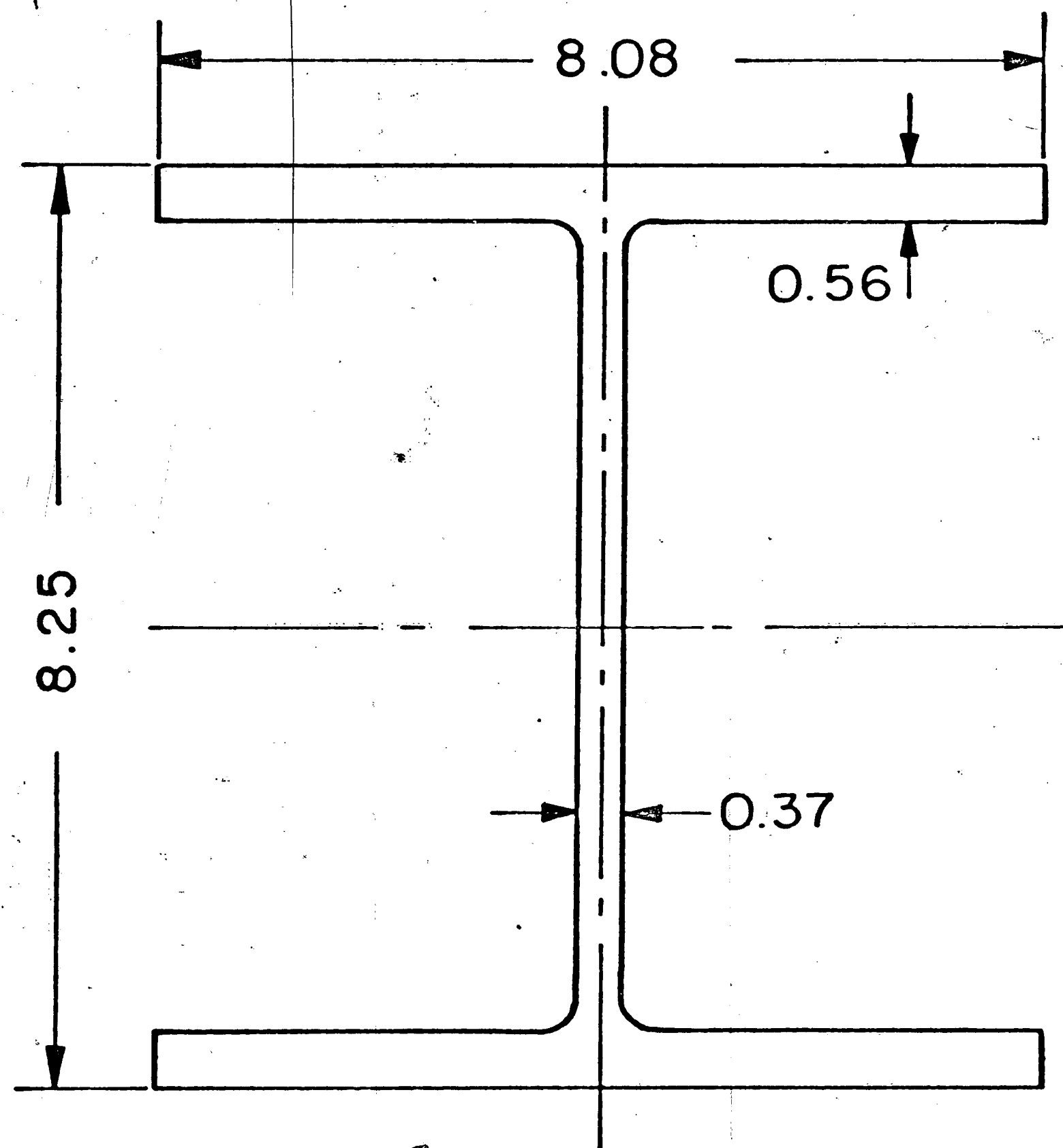
Heat No.	C	Mn	P	S	Si	Cr	Mo	Al	V	Cu	B	Ti	Sn
65A739	.18	.94	.009	.017	.27	.55	.17	.036	.06	---	.003	.02	---
66L739	.21	.90	.008	.018	.29	.60	.24	.037	.05	.25	.003	.02	0.001
72A655	.18	.85	.010	.026	.26	.55	.17	.025	.04	---	.003	.02	---

2. Mechanical Properties

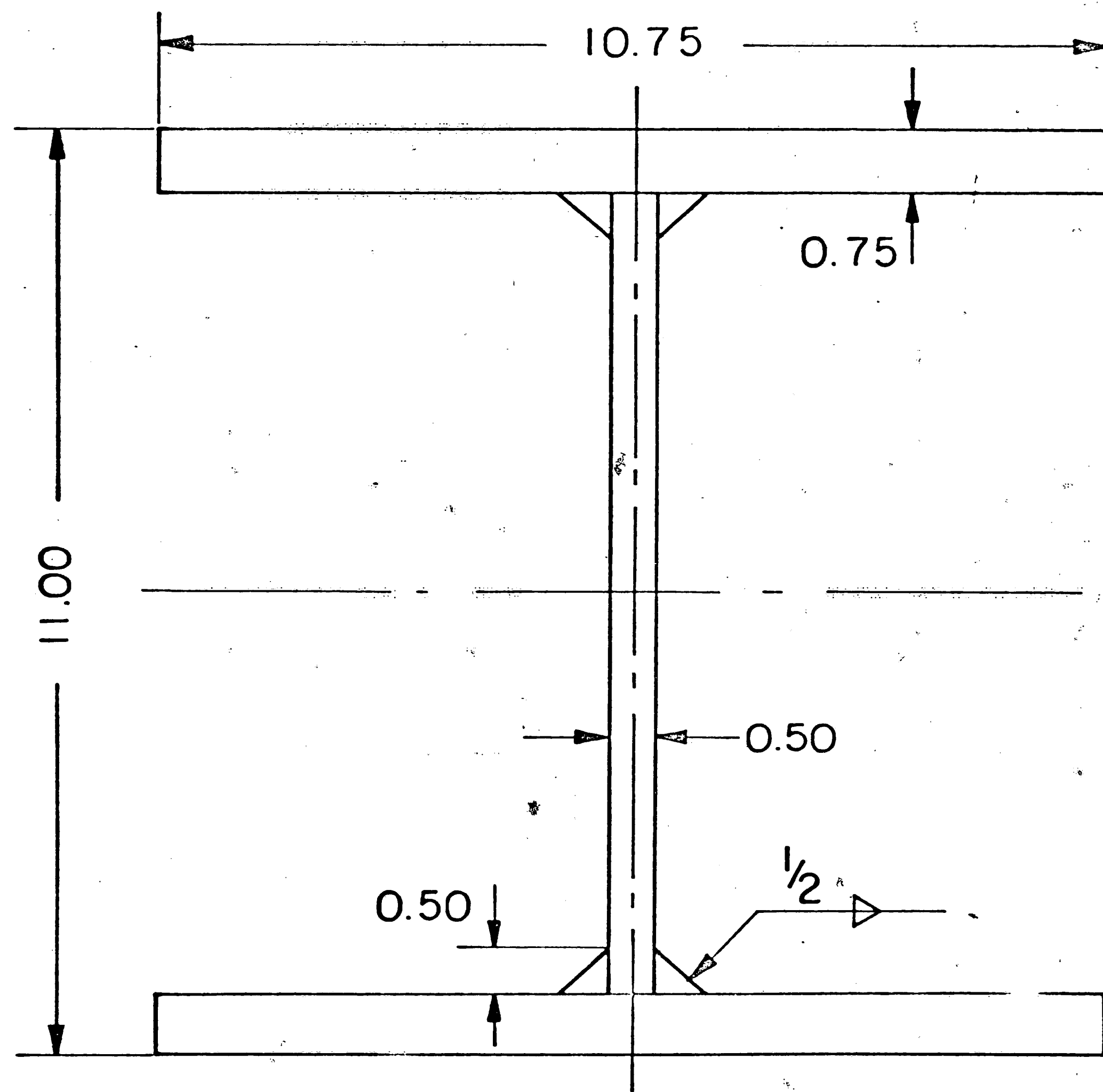
Heat No.	Tensile Strength psi	Yield Strength psi	Elongation in 2 in.	Percent Red. Area
65A739	122150	113800	22.0	61.6
66L739	124200	114400	36.0	58.7
72A655	125500	119000	31.0	51.4

TABLE 3 · SUMMARY OF TENSION COUPON TEST DATA

Designation	Dimensions Thickness(in) x Width(in)	E Young's Modulus (ksi)	y Static Yield Stress (ksi)	u Ultimate Stress (ksi)	E st Strain Hardening Modulus (ksi)
8WF40A	0.388 x 1.498	29.5	108.0	118.6	103.0
8WF40A ₁	0.551 x 1.498	29.4	110.5	123.0	106.5
8WF40A ₂	0.552 x 1.497	27.7	113.8	126.0	135.0
8WF40A ₃	0.556 x 1.497	27.6	113.0	125.1	178.0
8WF40E	0.389 x 1.493	28.4	128.0	137.0	137.5
8WF40E ₁	0.555 x 1.491	26.8	127.5	139.0	87.0
8WF40E ₂	0.556 x 1.493	29.5	131.0	142.0	149.0
8WF40E ₃	0.558 x 1.494	29.0	131.0	141.6	128.5
11H66J-32	0.284 x 1.503	30.2	112.8	124.0	197.0
11H66J-31	0.282 x 1.504	28.4	113.8	124.8	141.5
11H66J-20	0.494 x 1.502	29.4	104.0	116.8	183.0
11H66J-11	0.281 x 1.501	28.4	113.8	124.8	141.5
11H66J-12	0.289 x 1.500	27.9	114.5	125.0	104.0



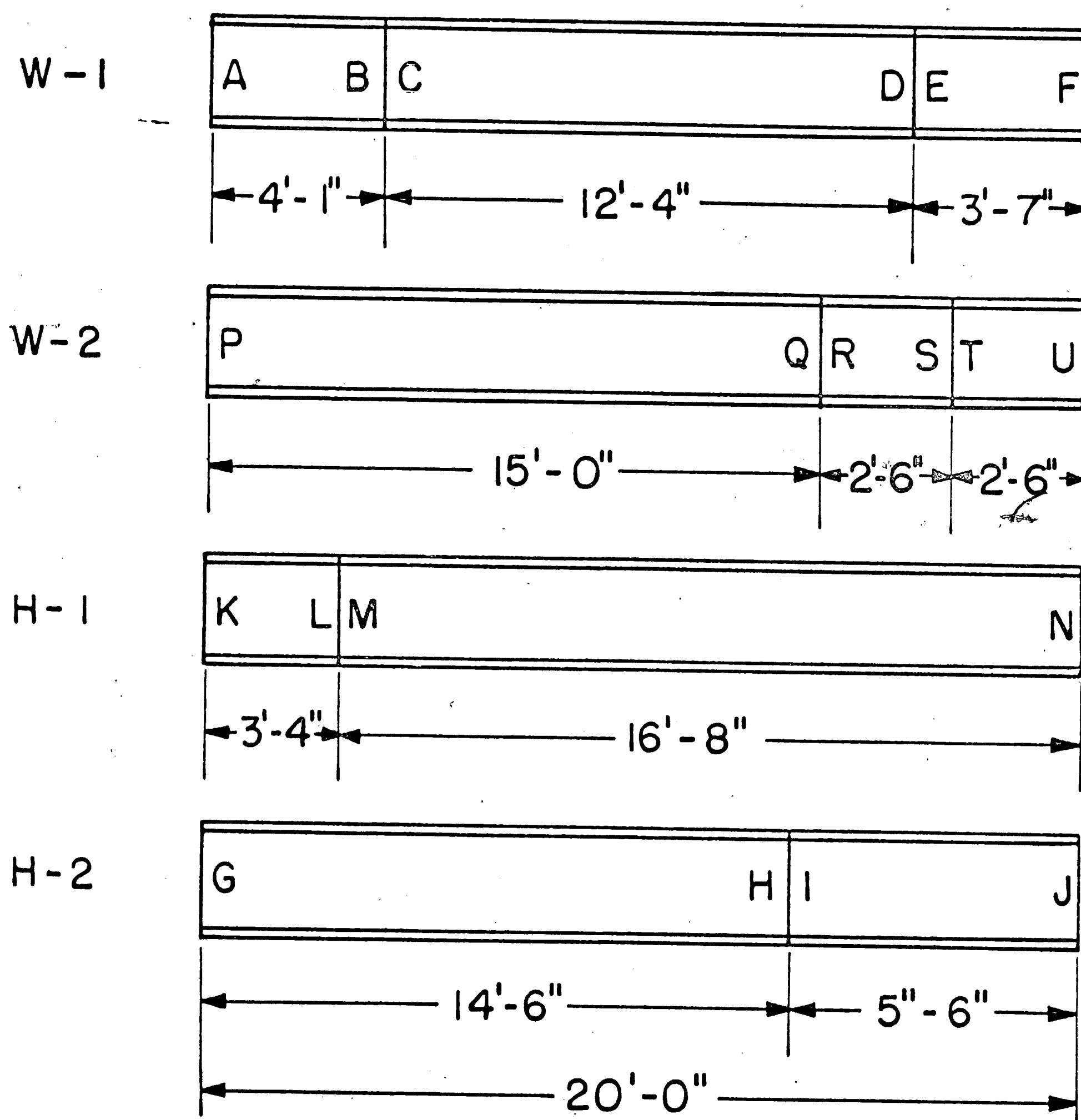
8W40



11H66

Fig. 1

Sections Investigated



W-1	AB	Stub Column and Coupons
	CD	Beam Column
	DE	Coupons and Residual Stresses
W-2	RS, TU	Moment Arms
H-1	MN	Beam Column
H-2	IJ	Coupons Residual Stresses and Stub Column
Others		Storage

Fig. 2

Specimen Layout

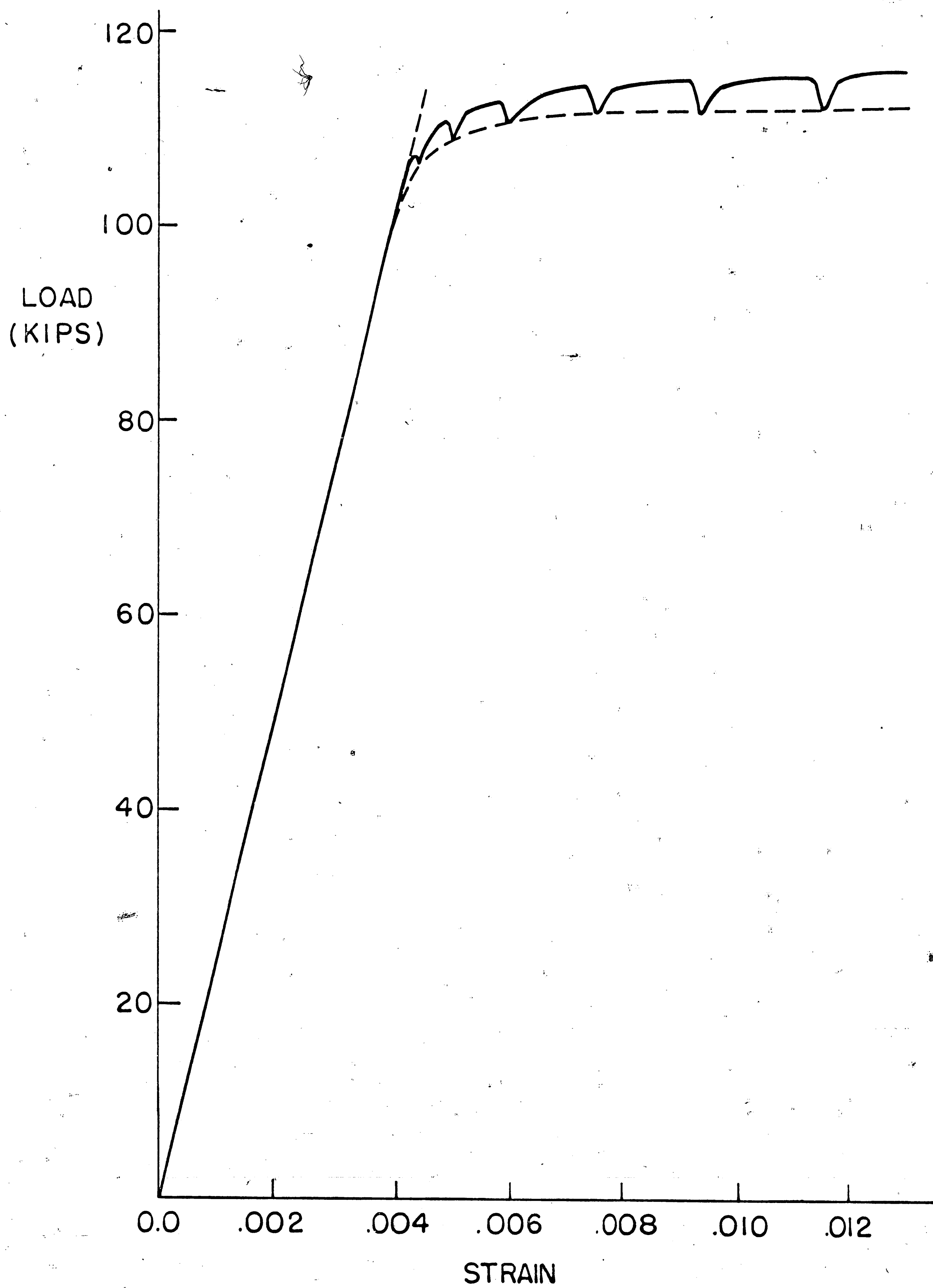


Fig. 3

Typical Coupon Test Data

STRESS AND STRAIN RELATIONSHIP

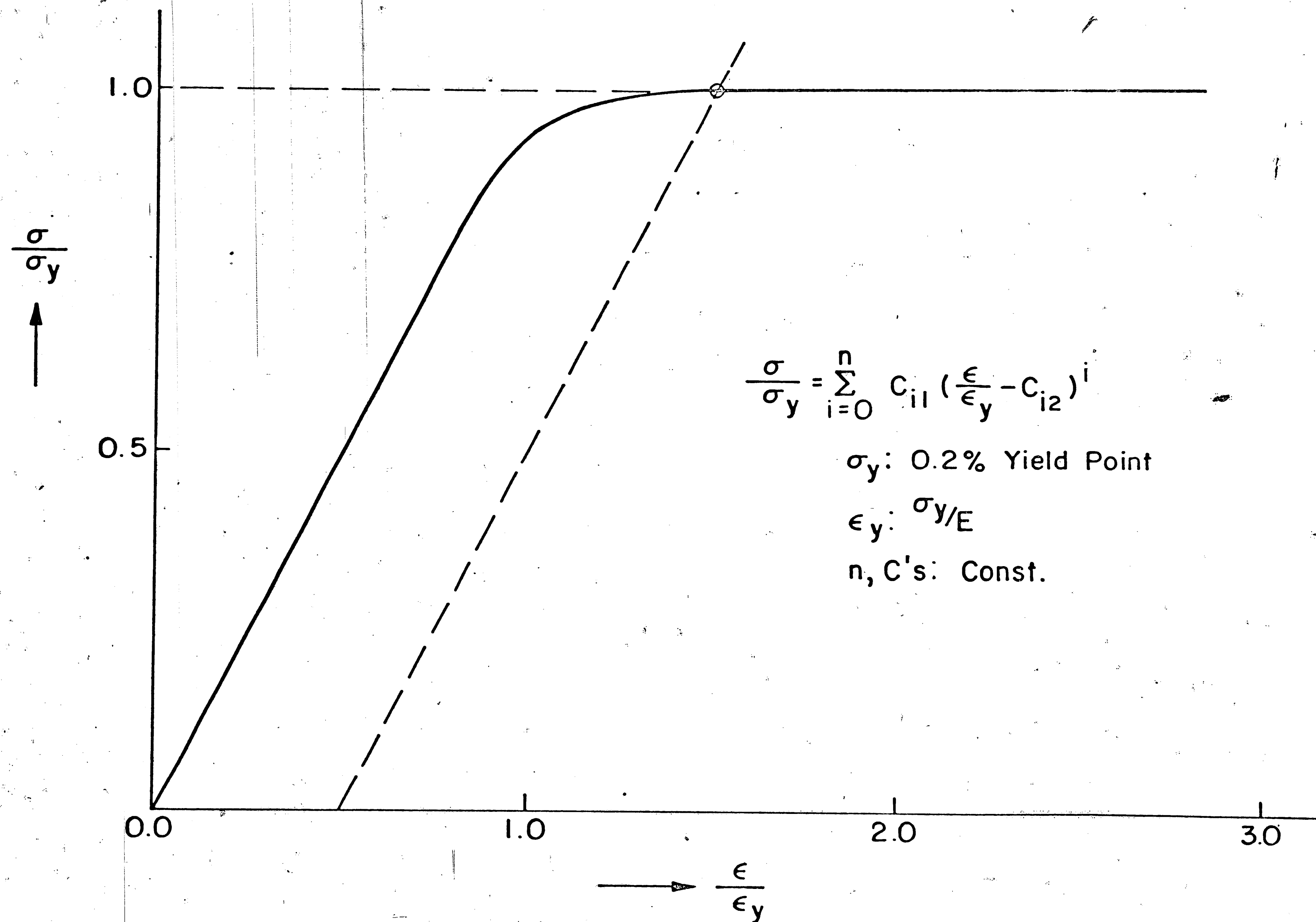


Fig. 4

Summarized Stress-Strain Relationship

RESIDUAL STRESSES

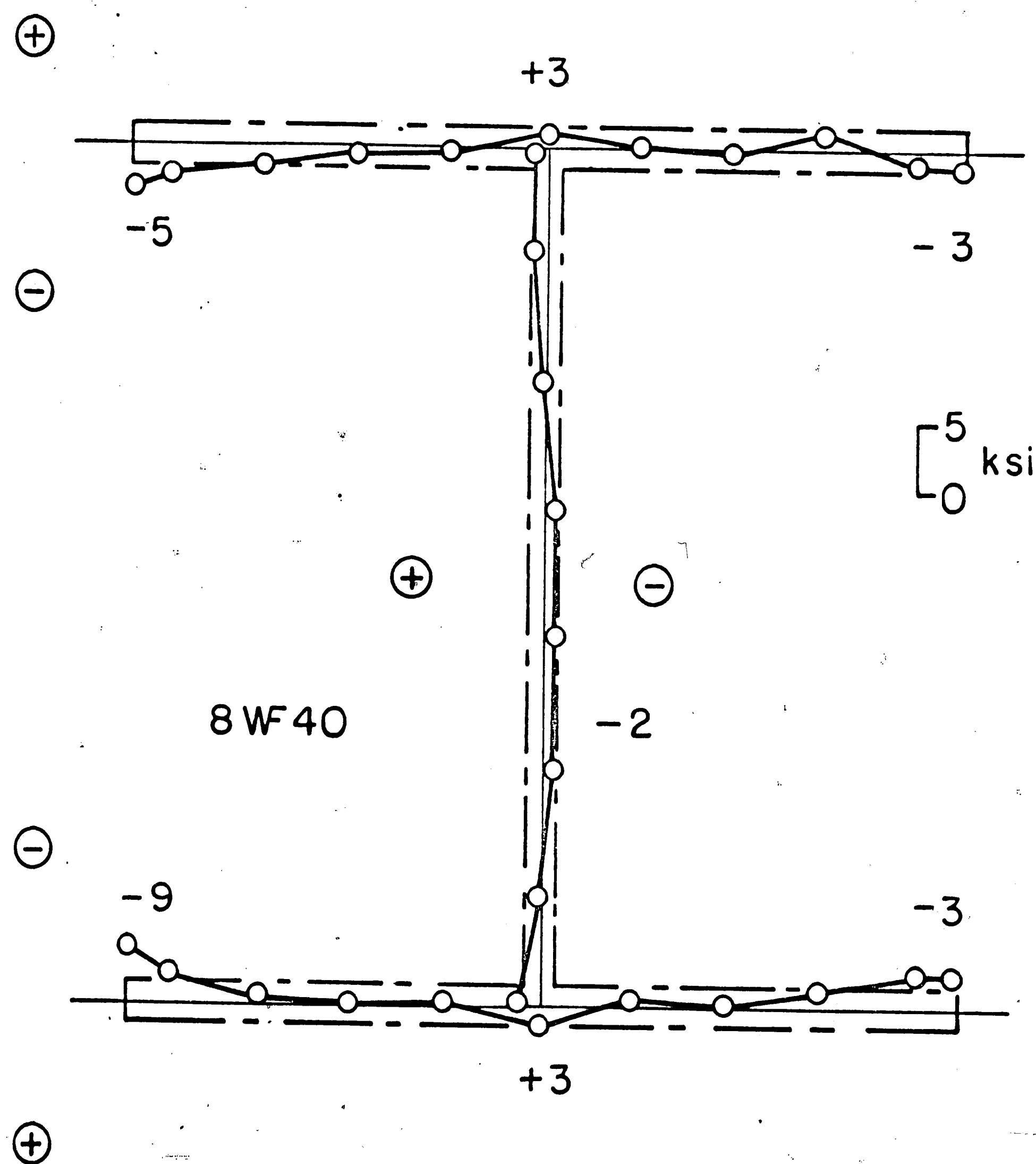


Fig. 5 Residual Stresses in 8WF40 Section

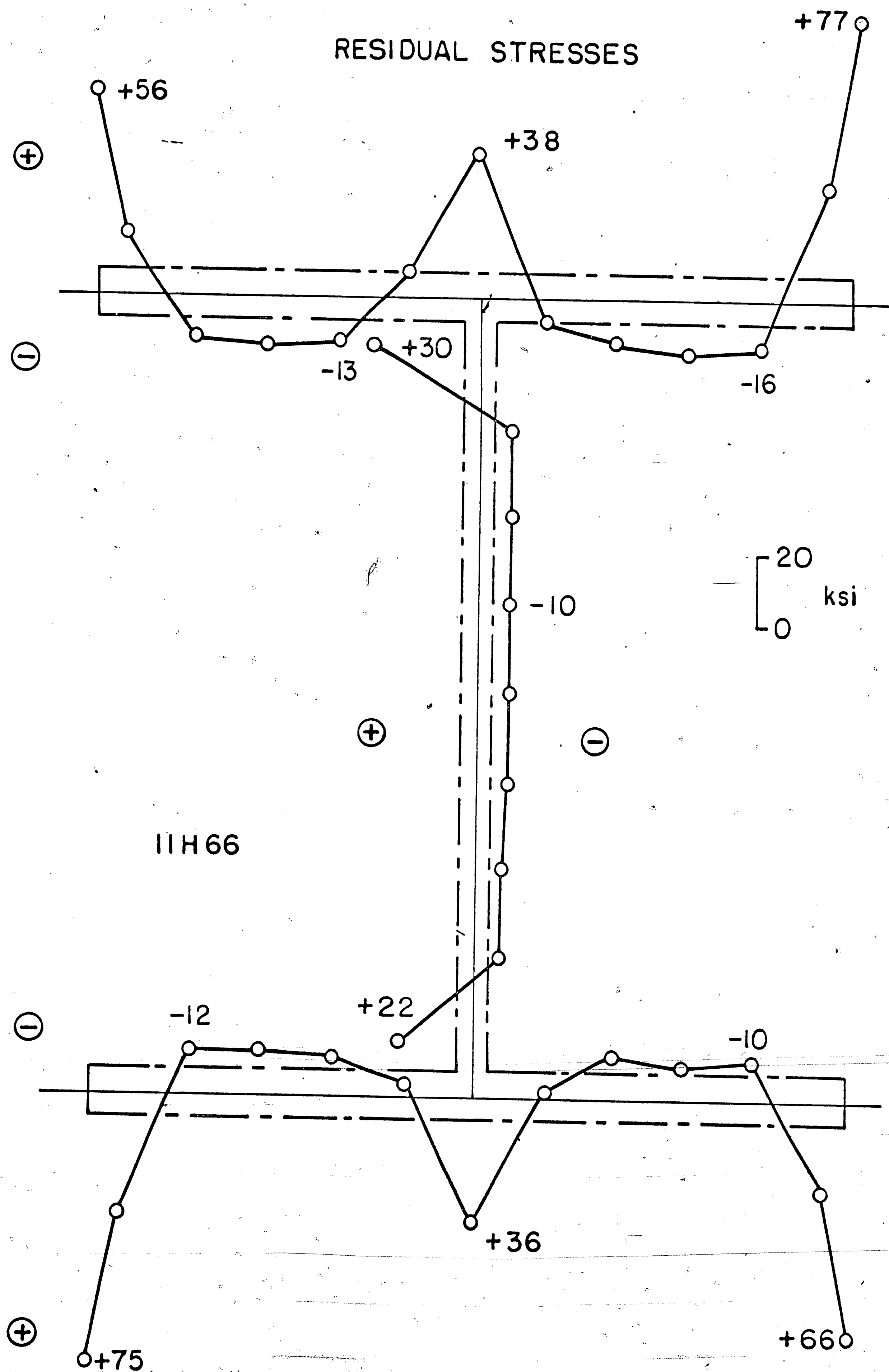


Fig. 6

Residual Stresses in 11H66 Section

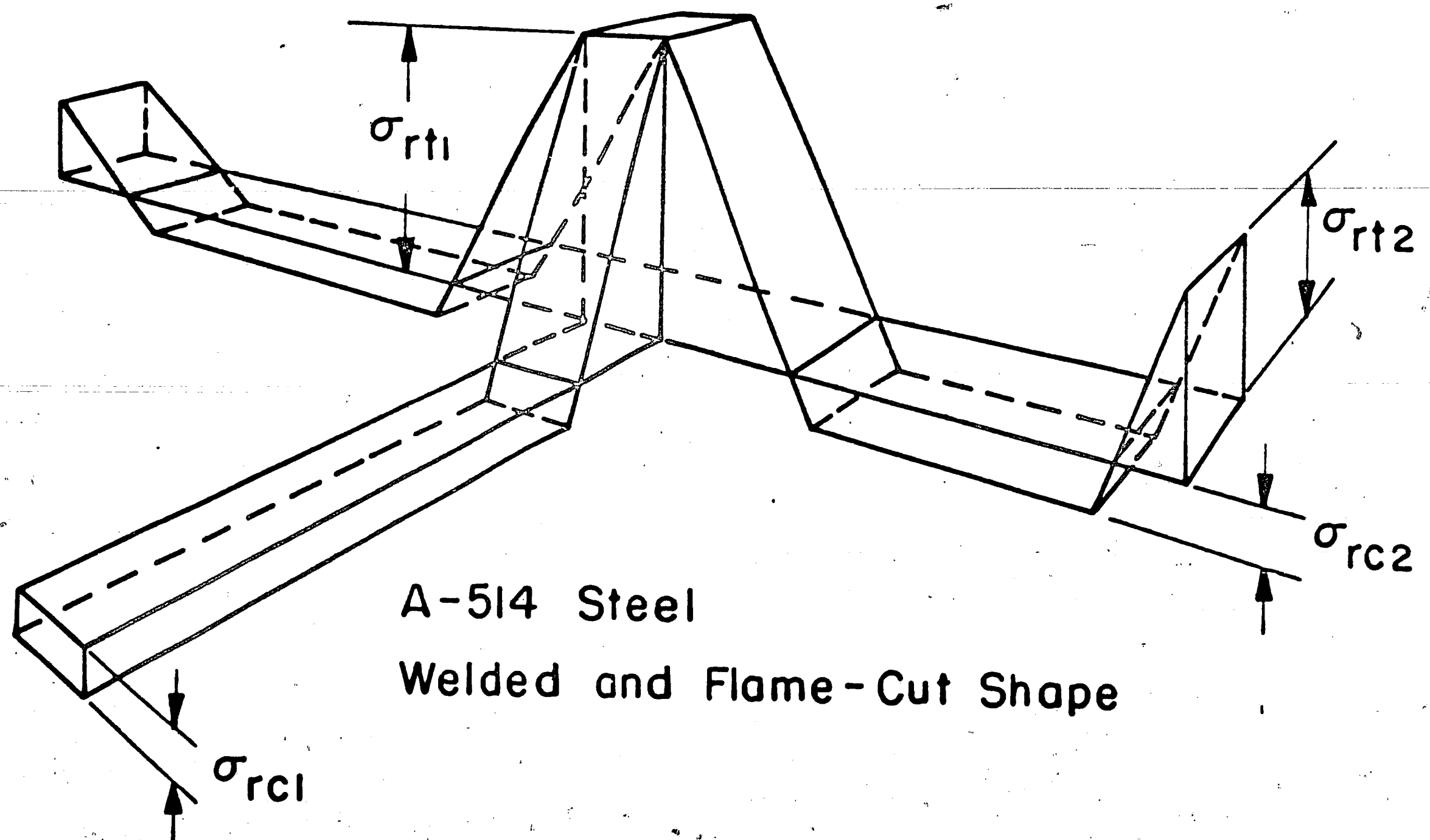
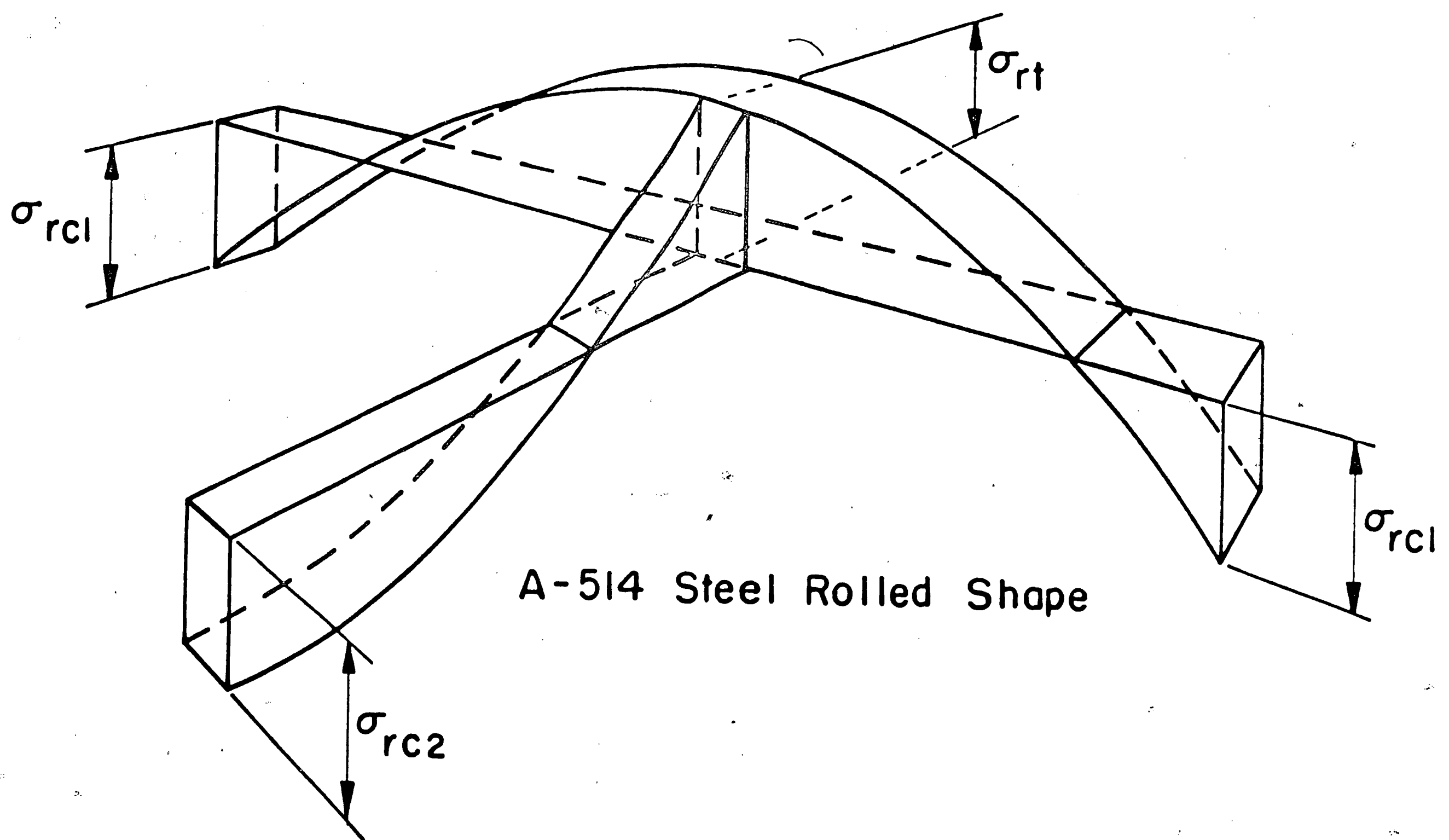
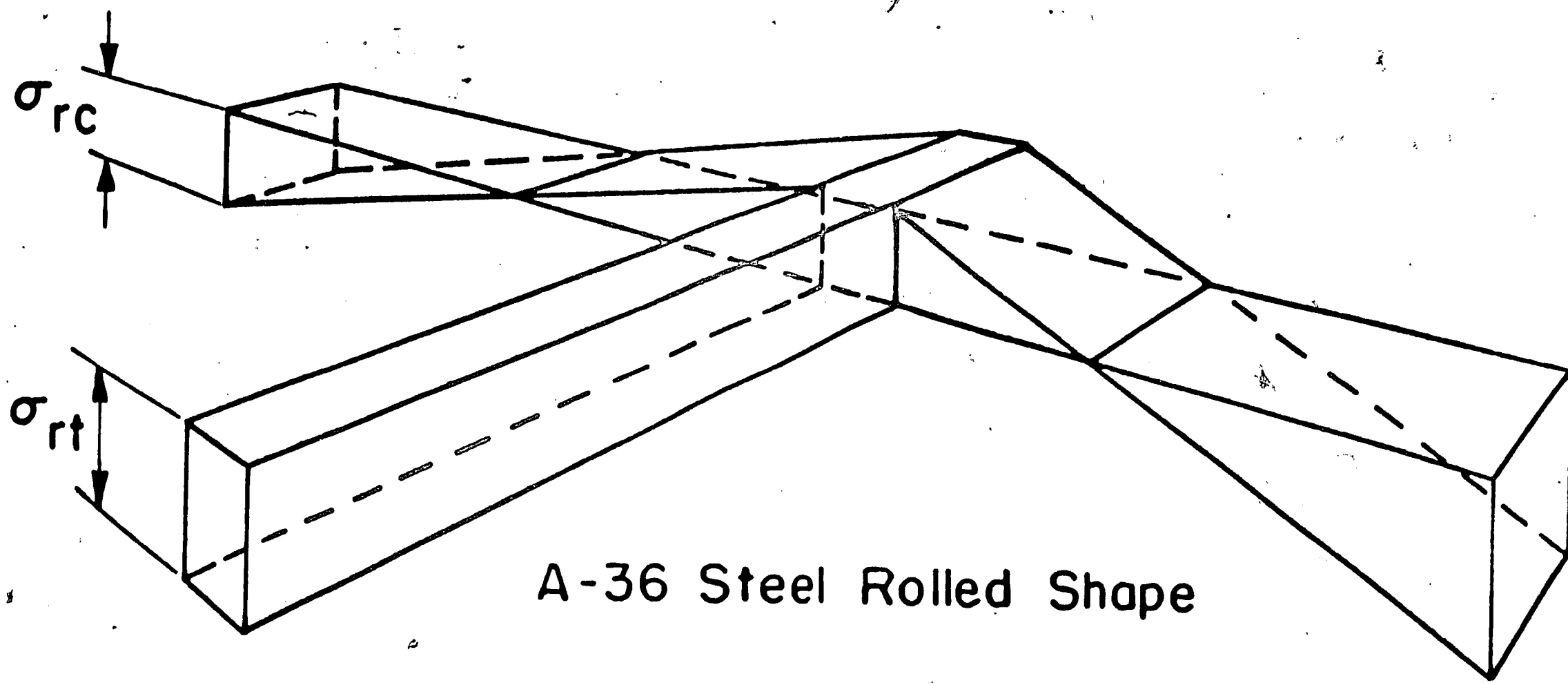


Fig. 7

Typical Residual Stress Patterns

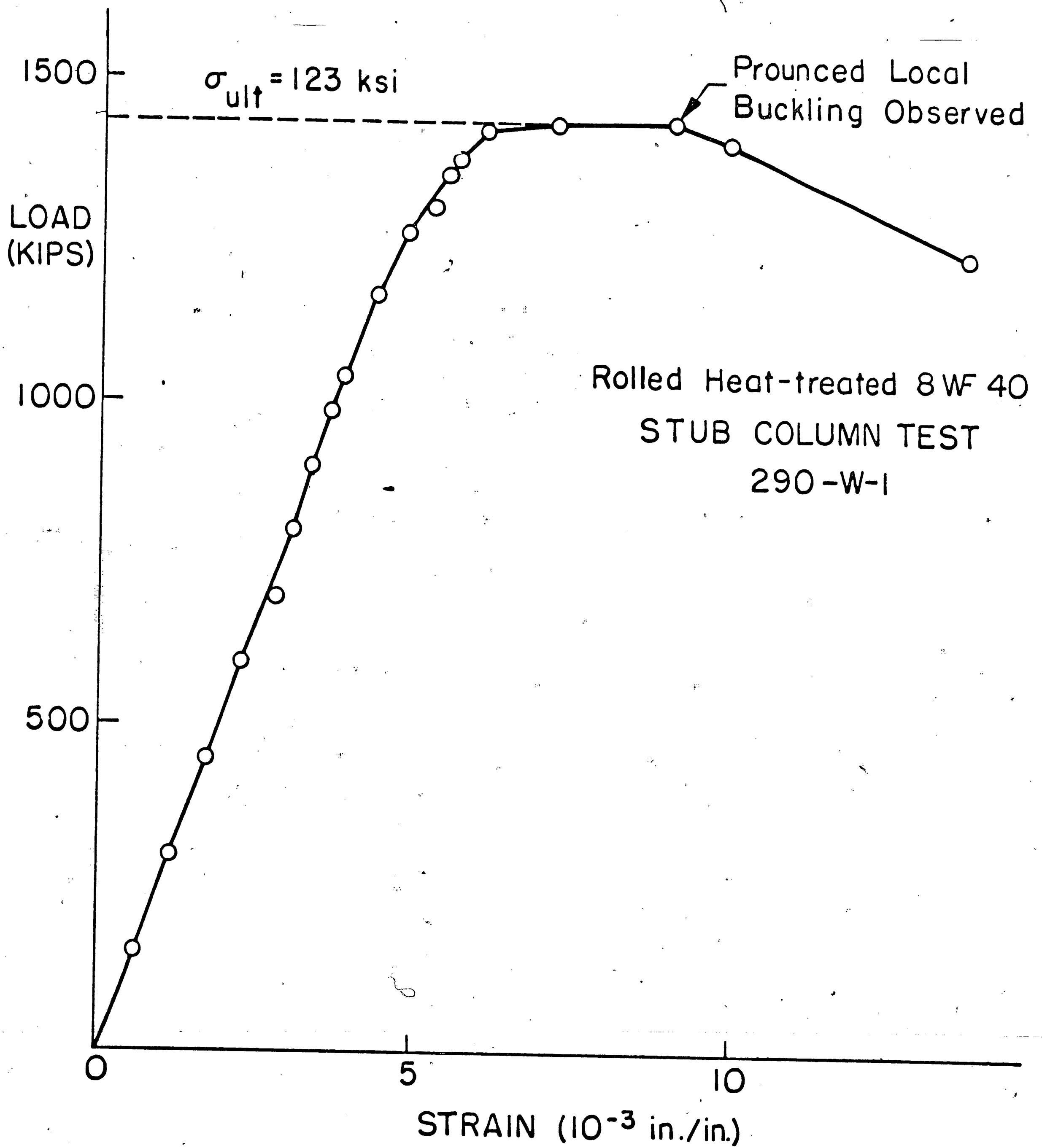


Fig. 8

Stub Column Test for 8WF40 Section

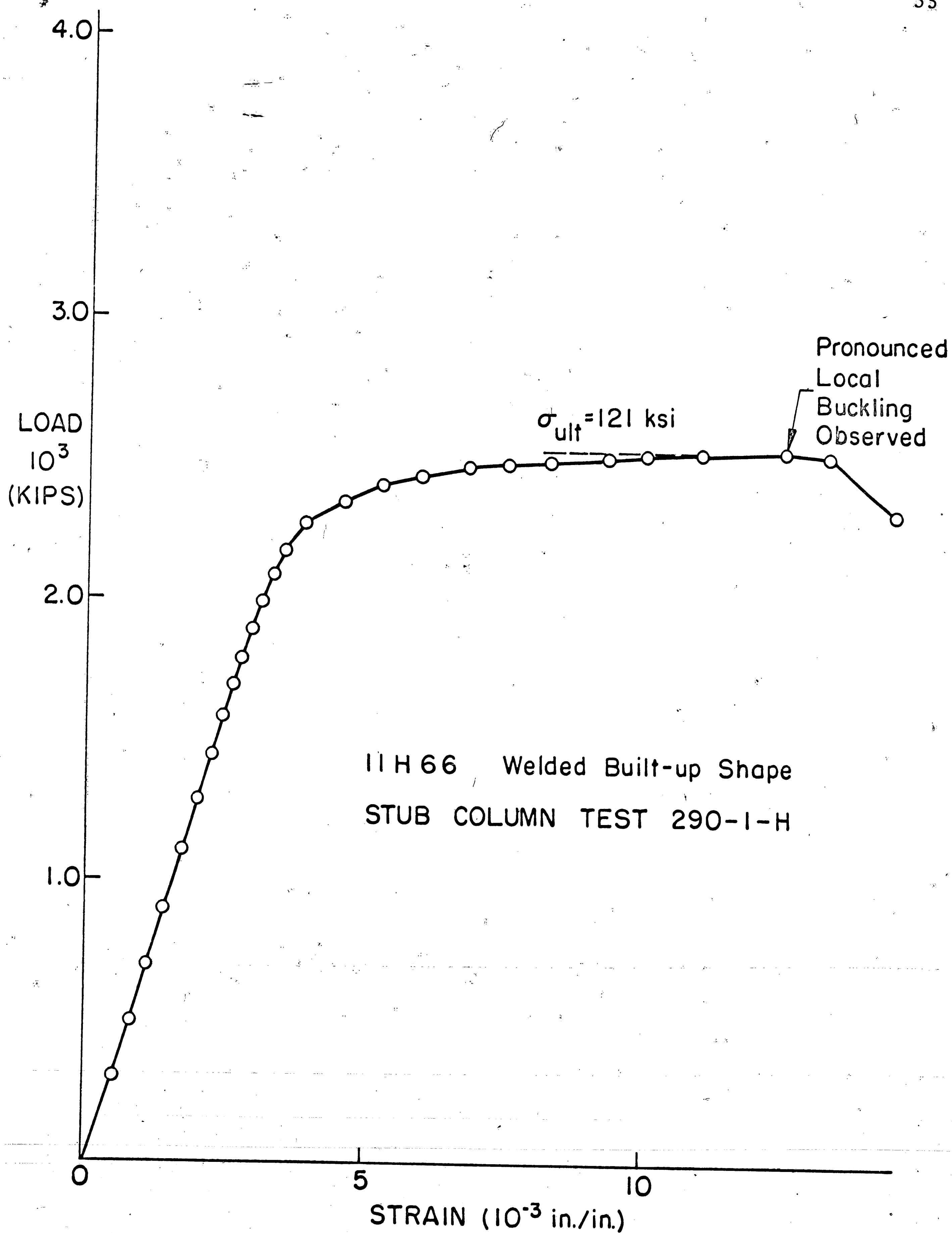
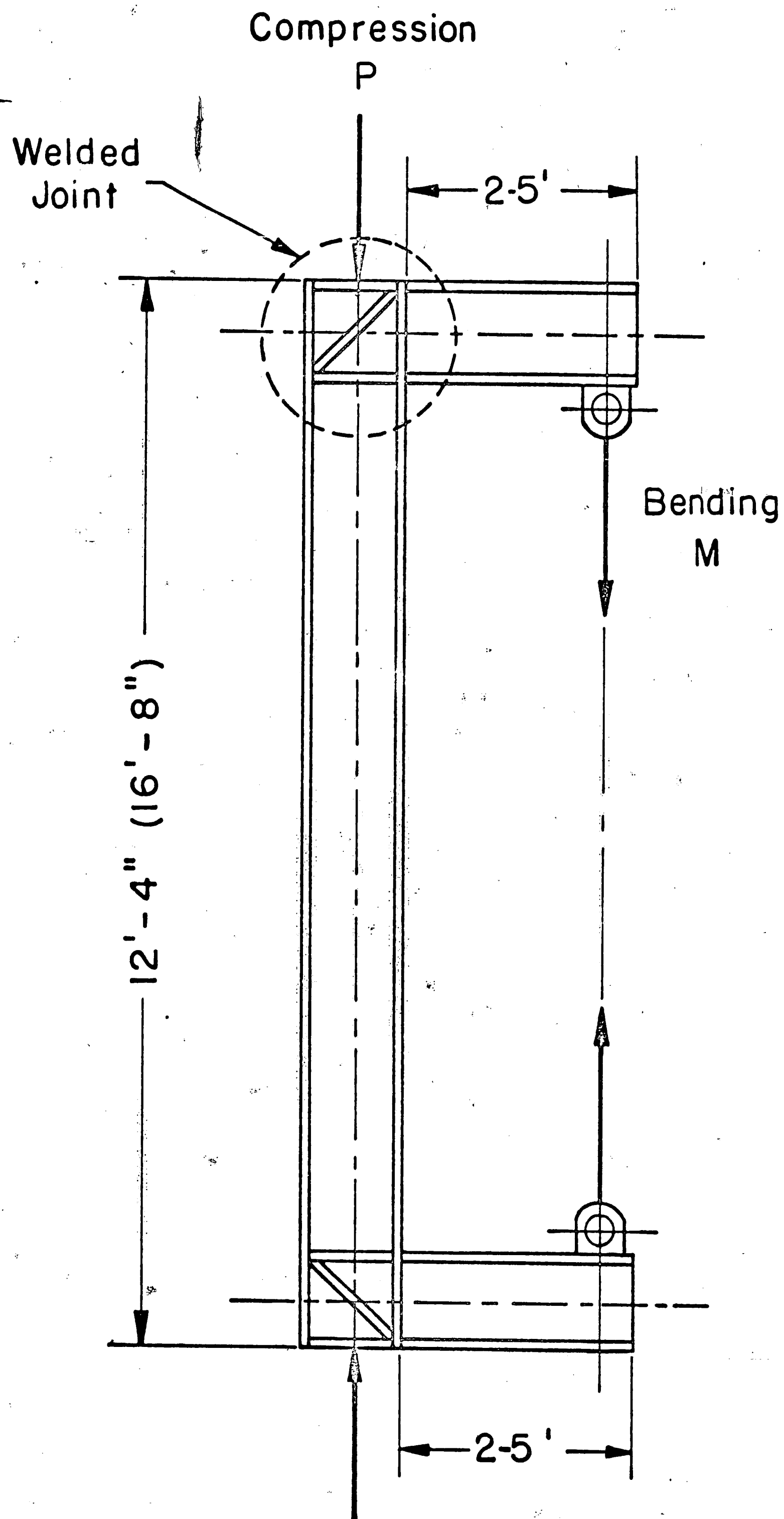


Fig. 9

Stub Column Test for 11H66 Section



SPECIMENS' LAYOUT

Fig. 10

General Layout of Specimen

A SCHEMATIC OF LOAD APPLICATION

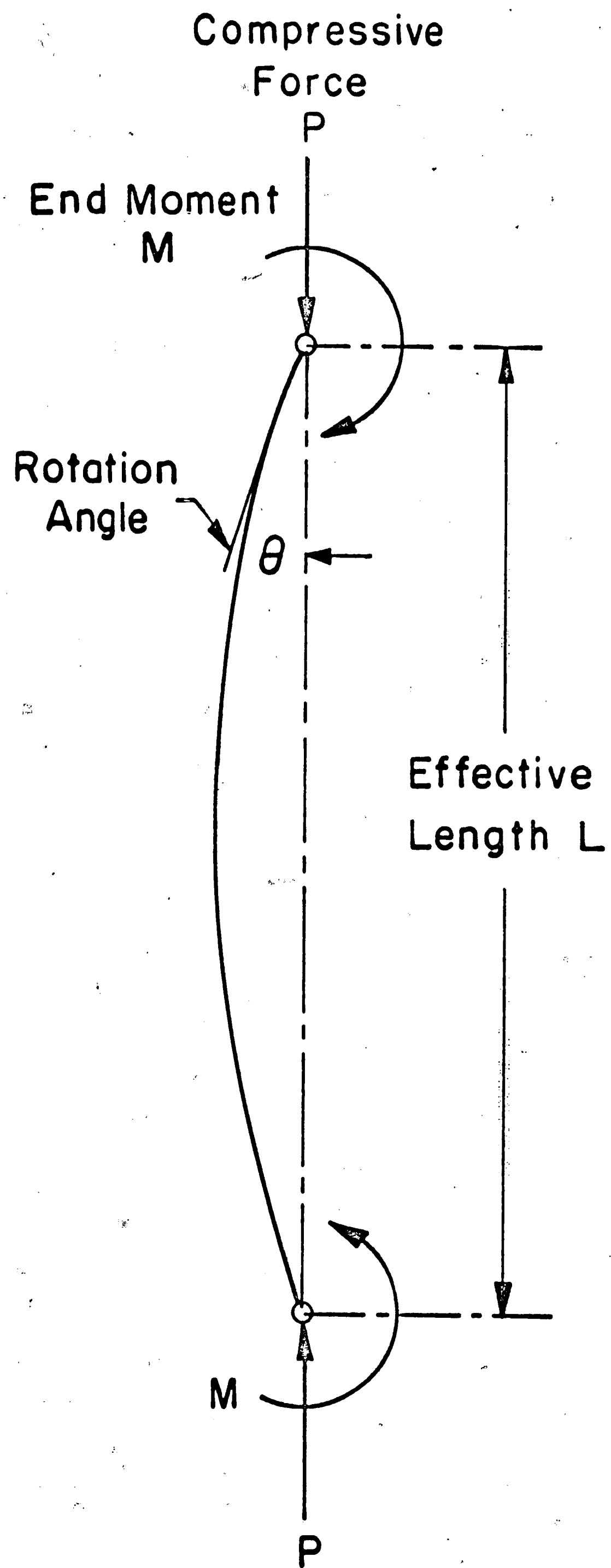


Fig. 11 Schematic Representation of Load Application

MECHANISM OF LATERAL BRACING

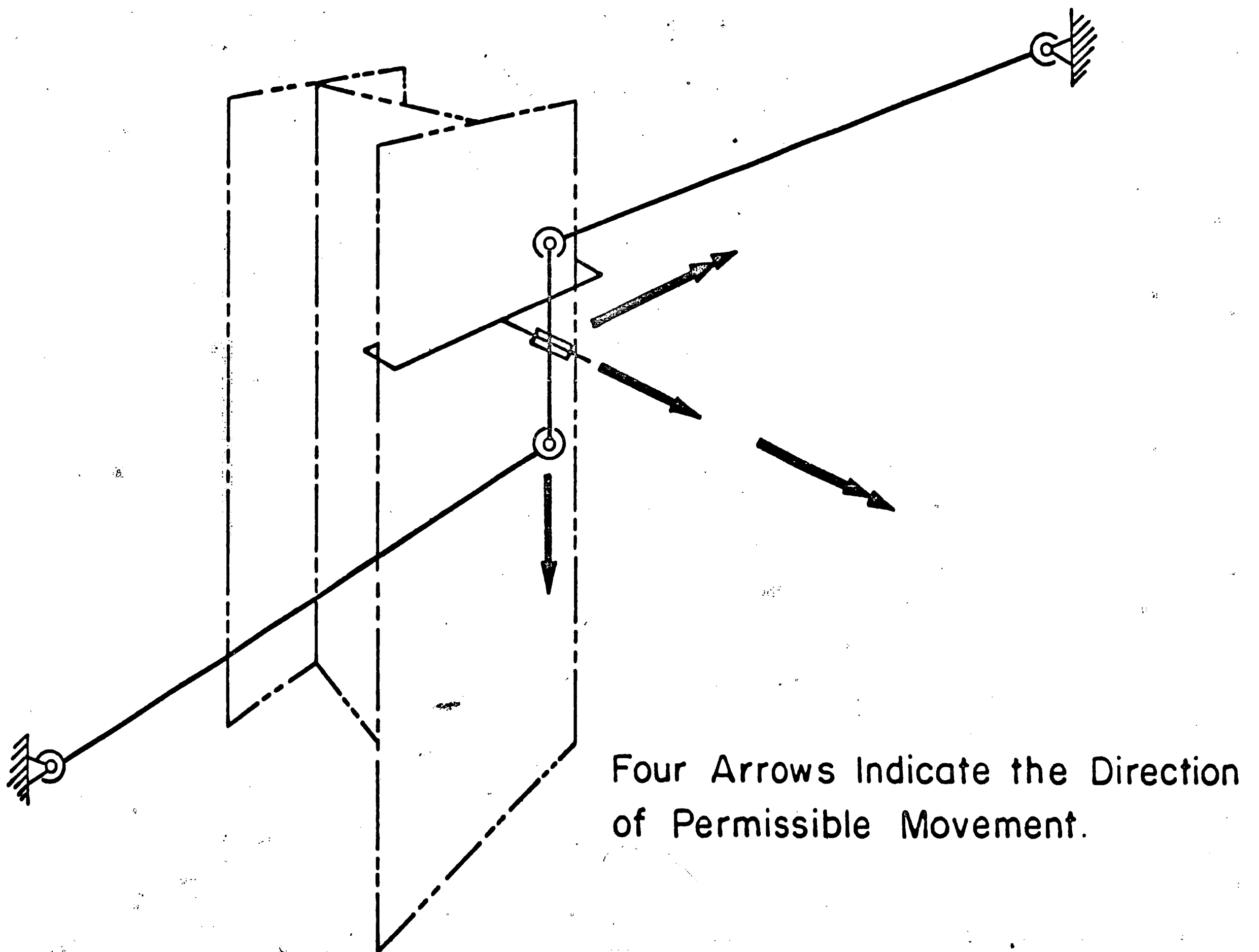
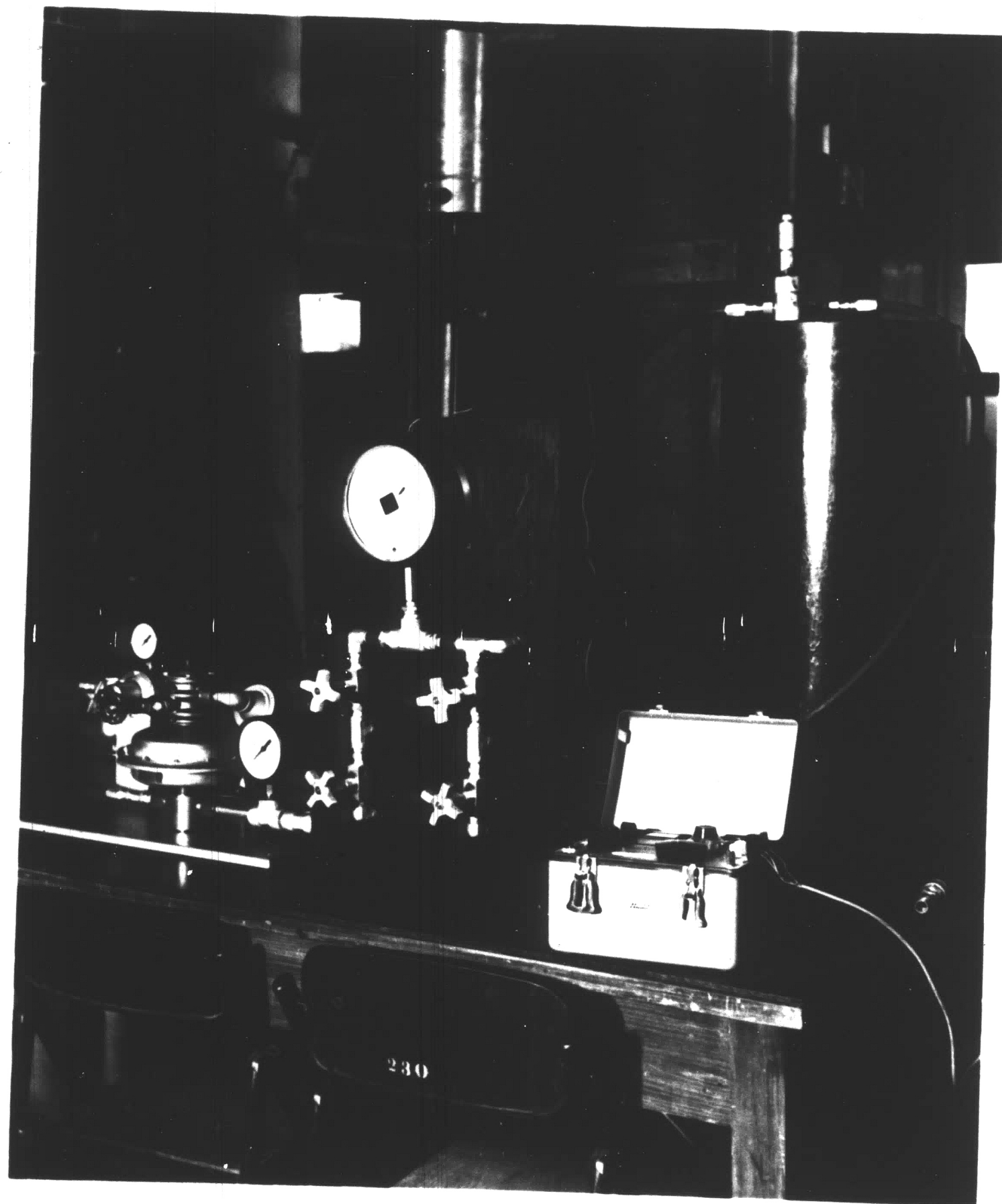


Fig. 12 Mechanism of Lateral Bracing

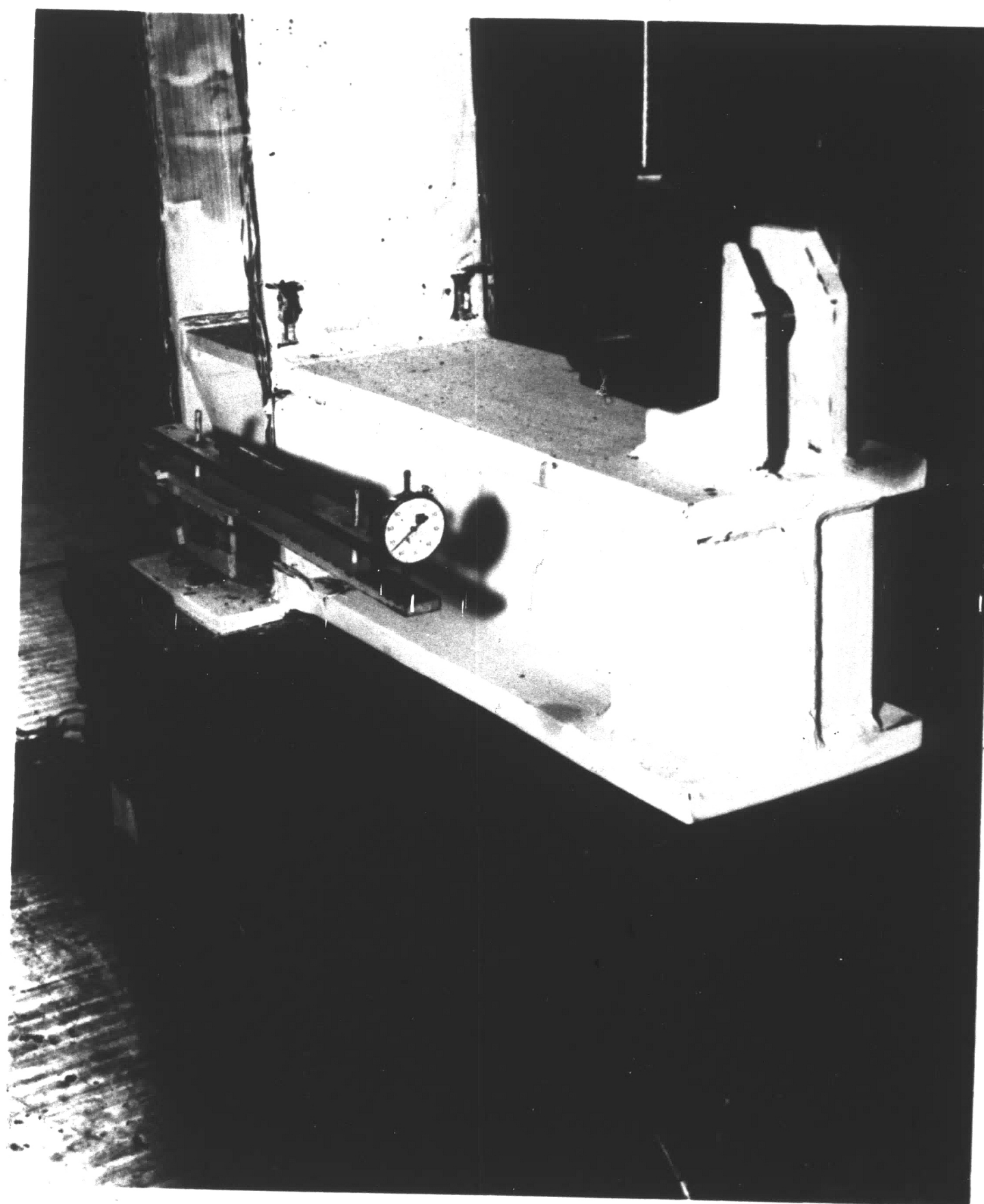


(a) General Test Setup

Fig. 13 Test Setup



(b) Jack Pressure Converter



(c) End Rotation Gage

INSTRUMENTS LAYOUT

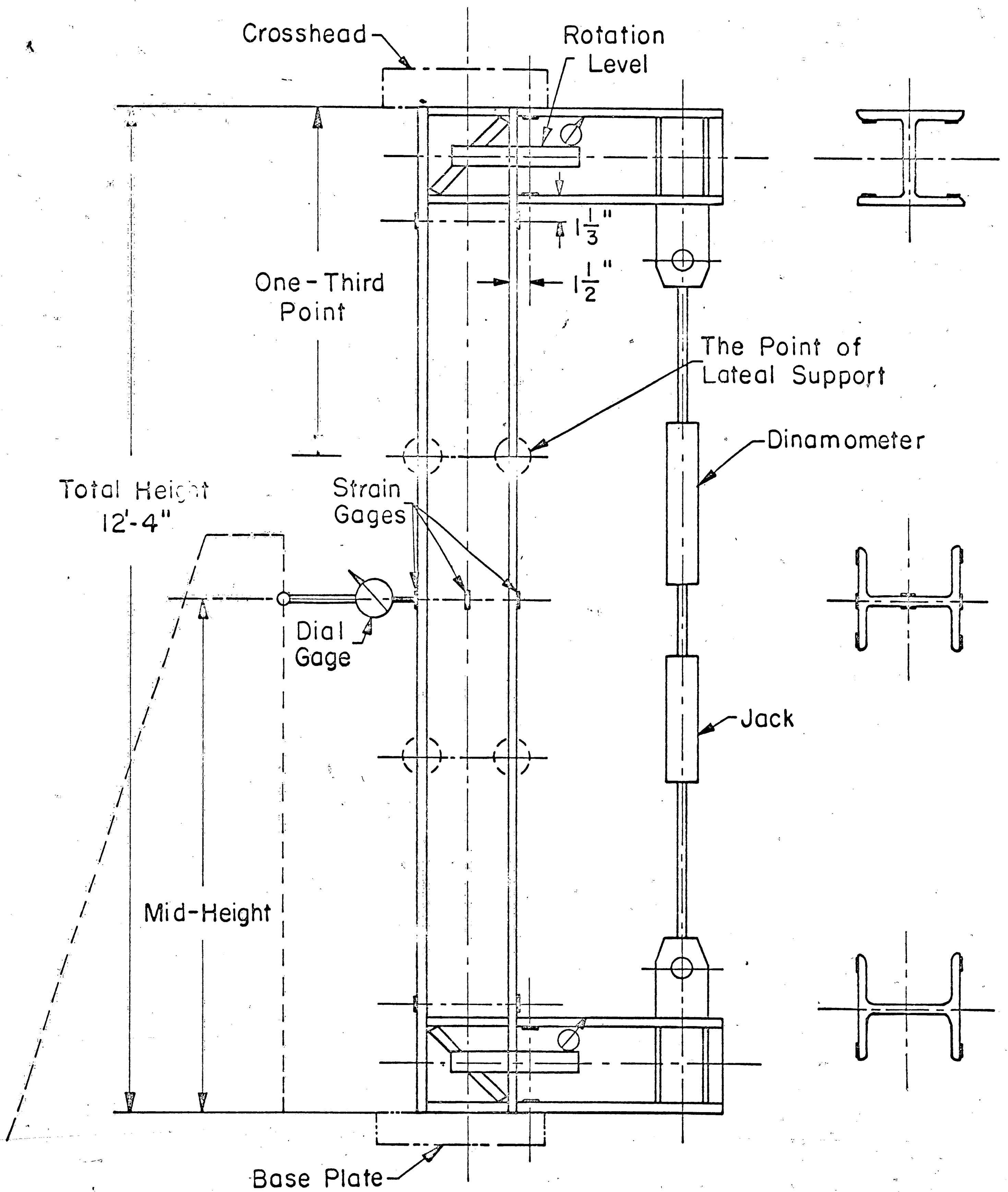


Fig. 14

Instrument Layout

BEAM COLUMN TEST

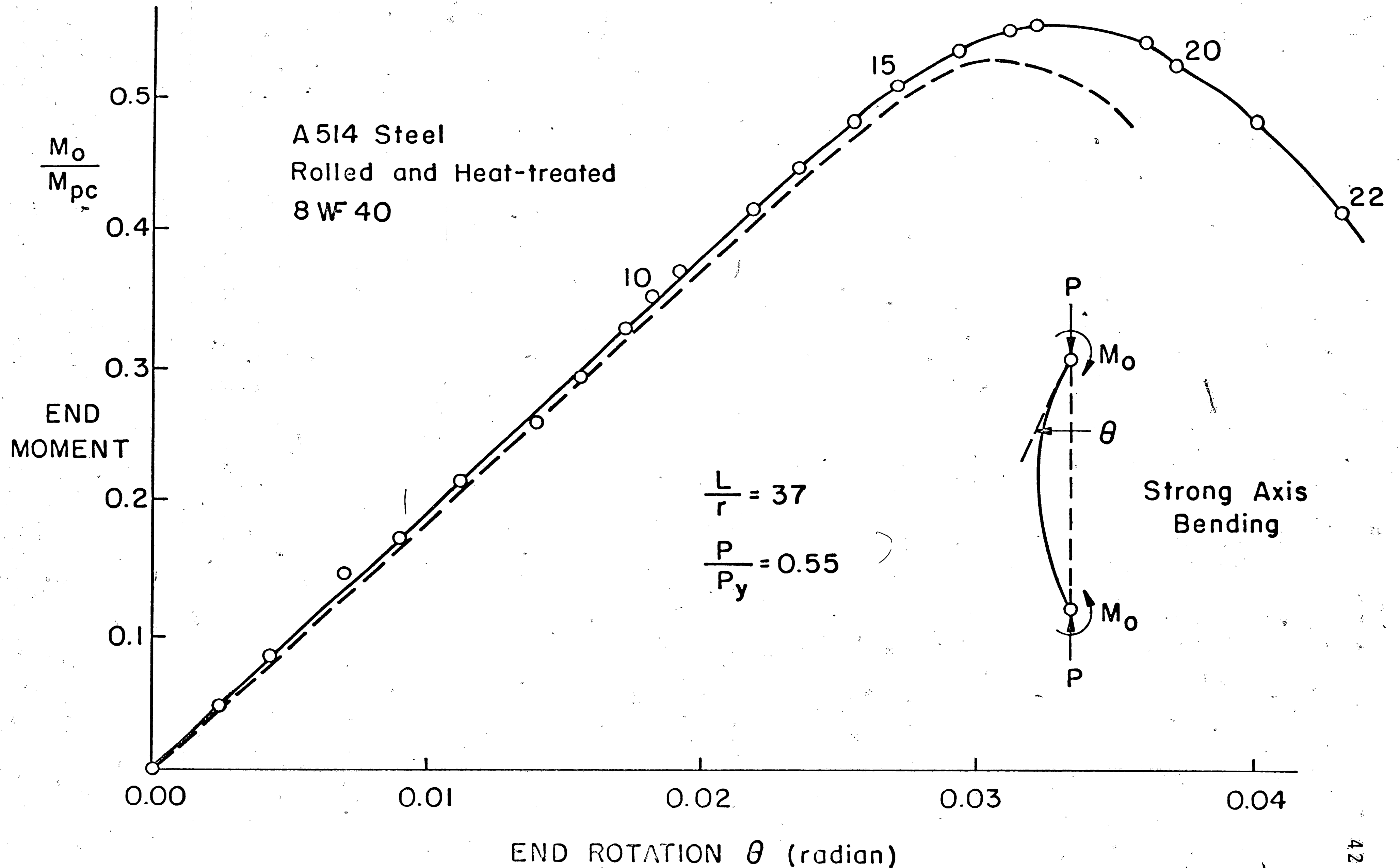


Fig. 15 Behavior of 8WF40 Beam-Column

BEAM COLUMN TEST

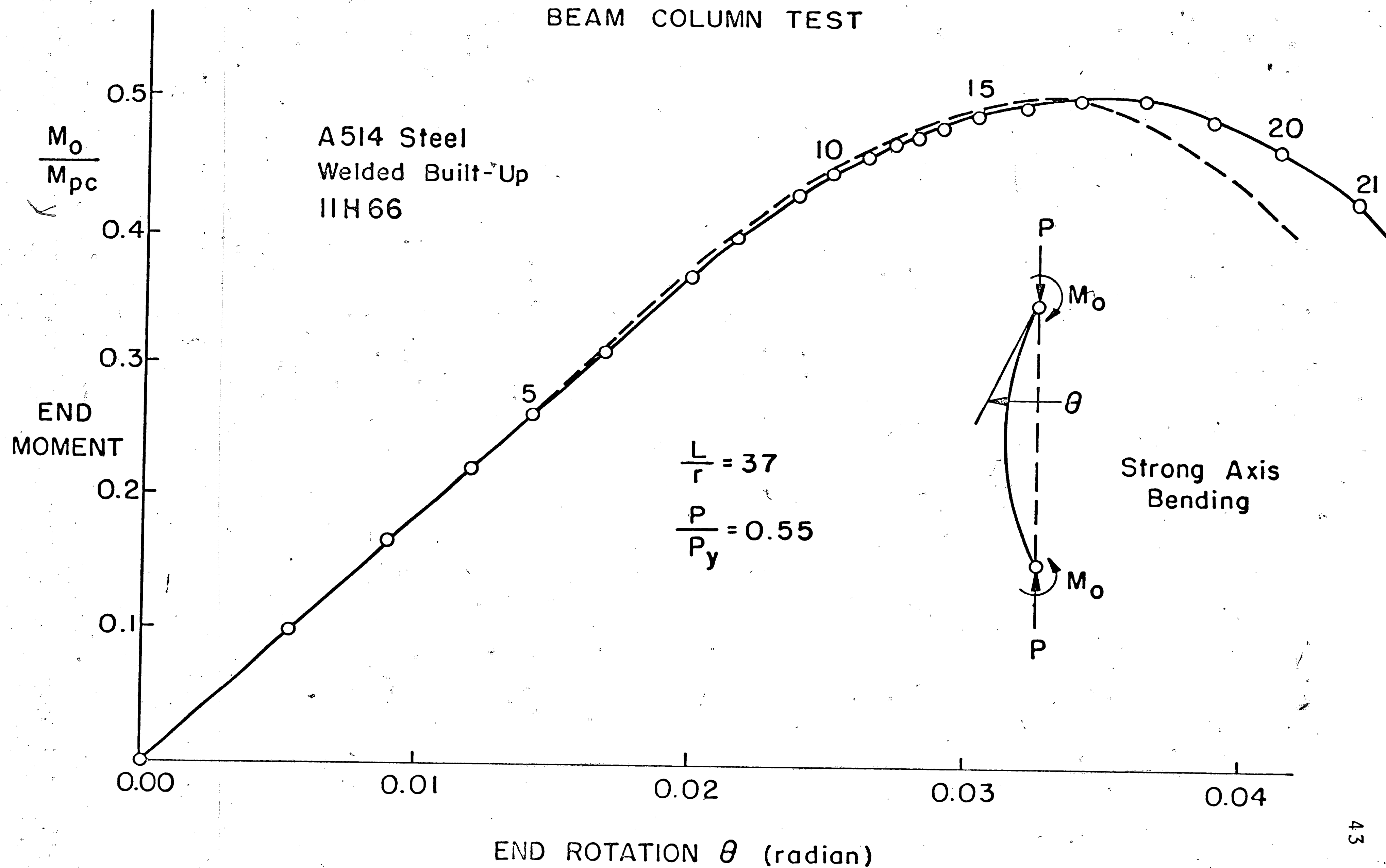


Fig. 16

Behavior of I1H66 Beam-Column

END MOMENT AND MID-HEIGHT DEFLECTION

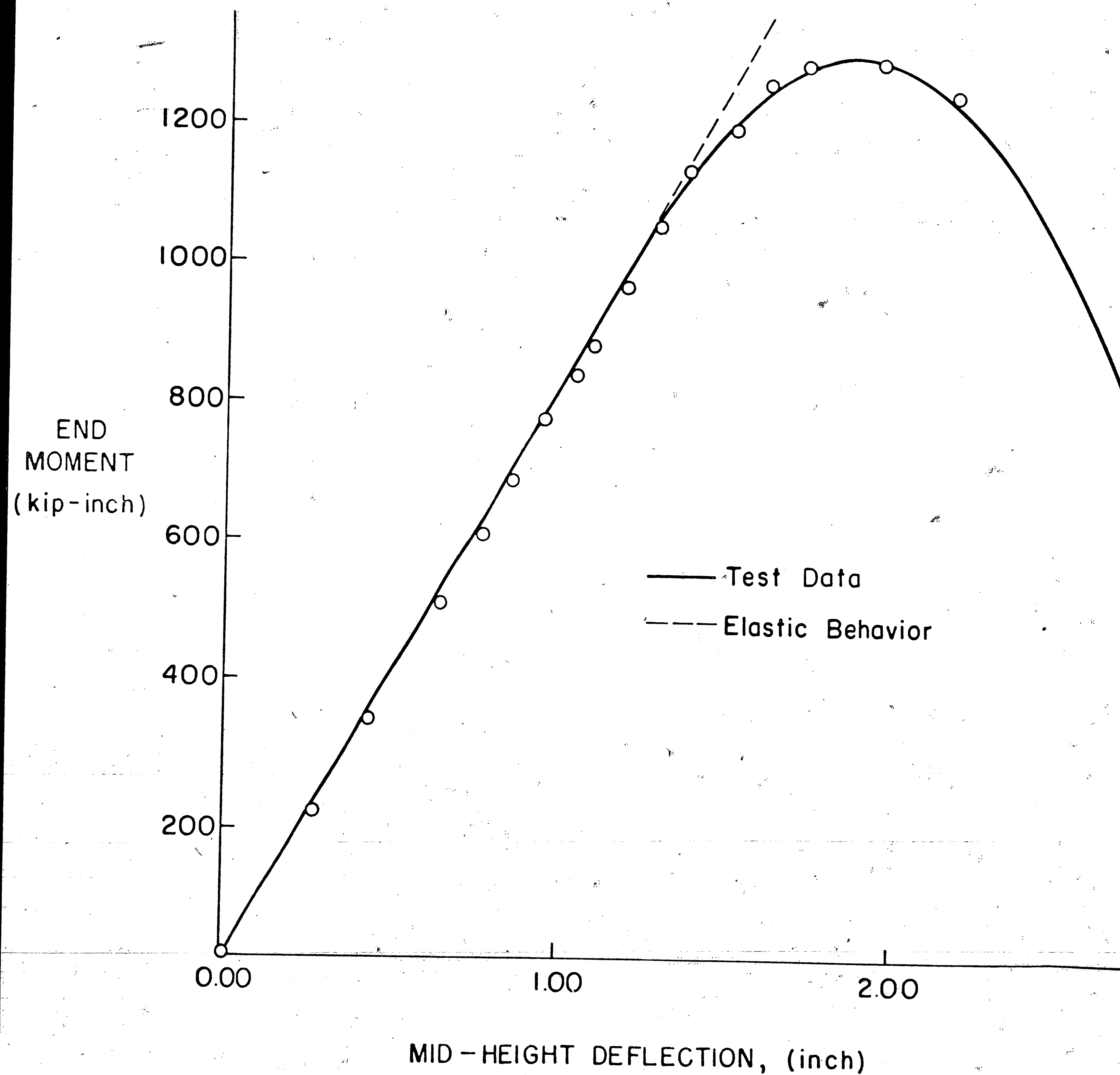


Fig. 17

Moment Deflection Curve, 8WF40 Beam-Column

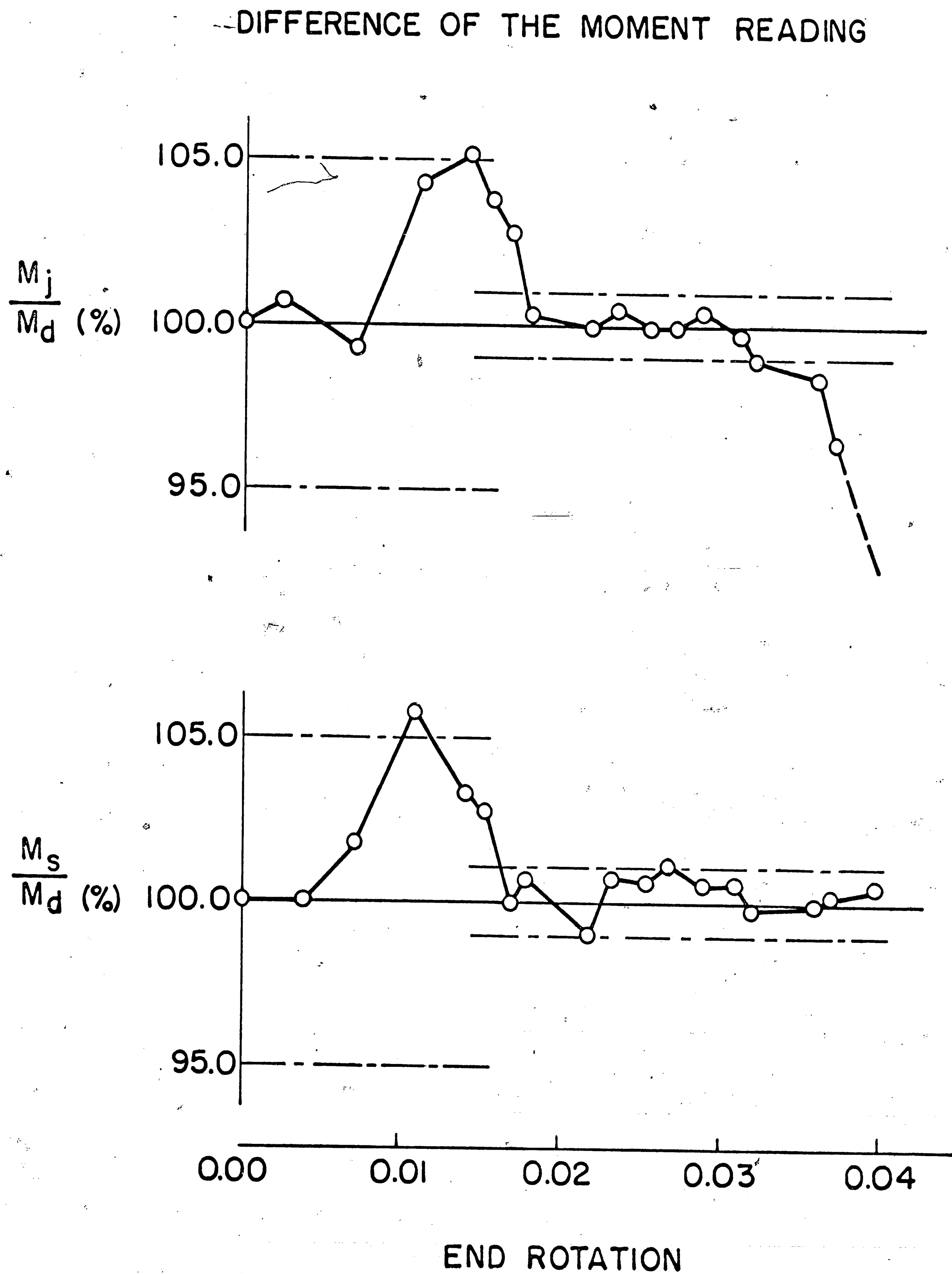


Fig. 18

Difference of the Moment Reading

LOCAL BUCKLING BEHAVIOR

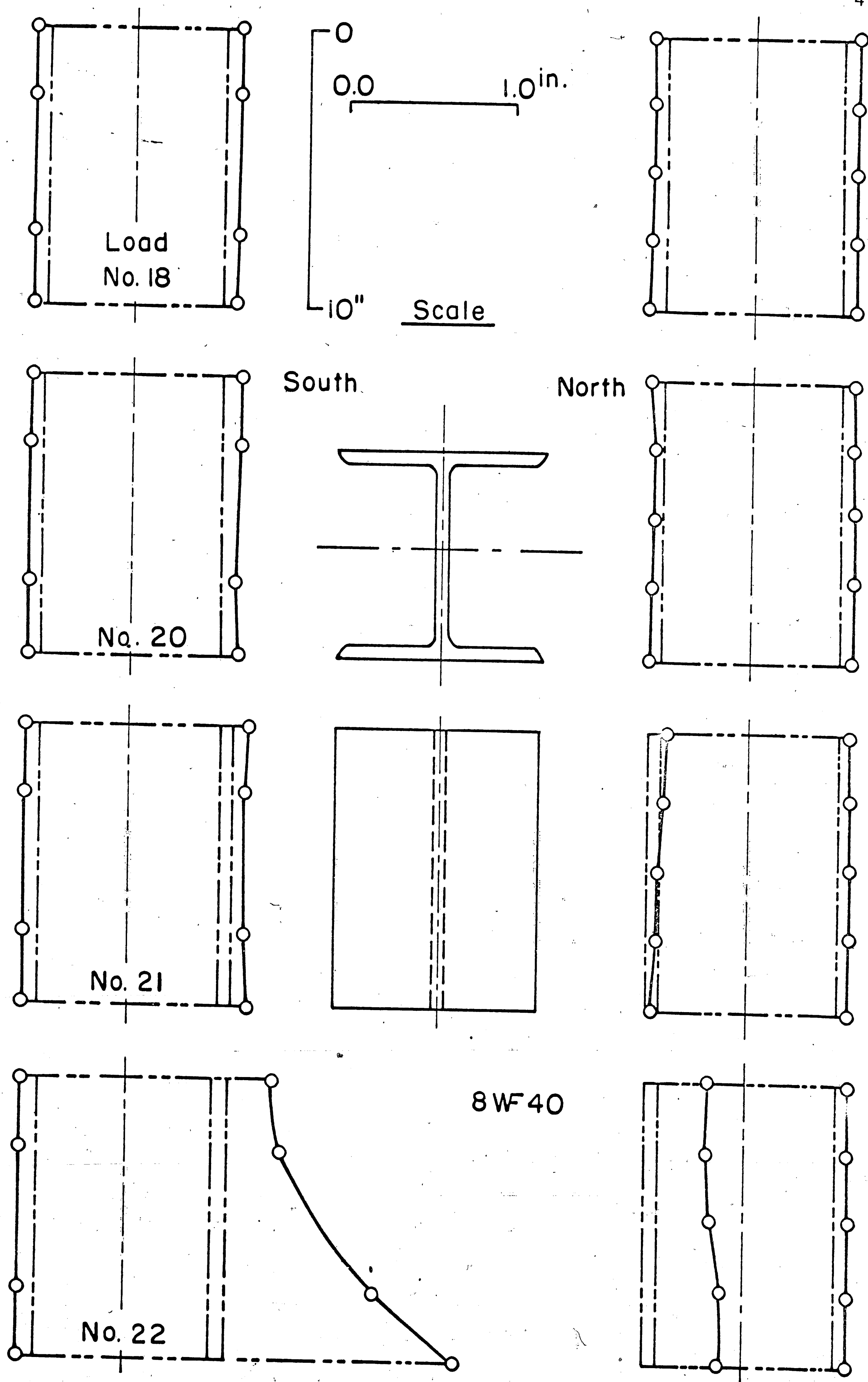


Fig. 19 Local Buckling Behavior, 8WF40



Fig. 20

Failure Mode, 8WF40 Beam-Column

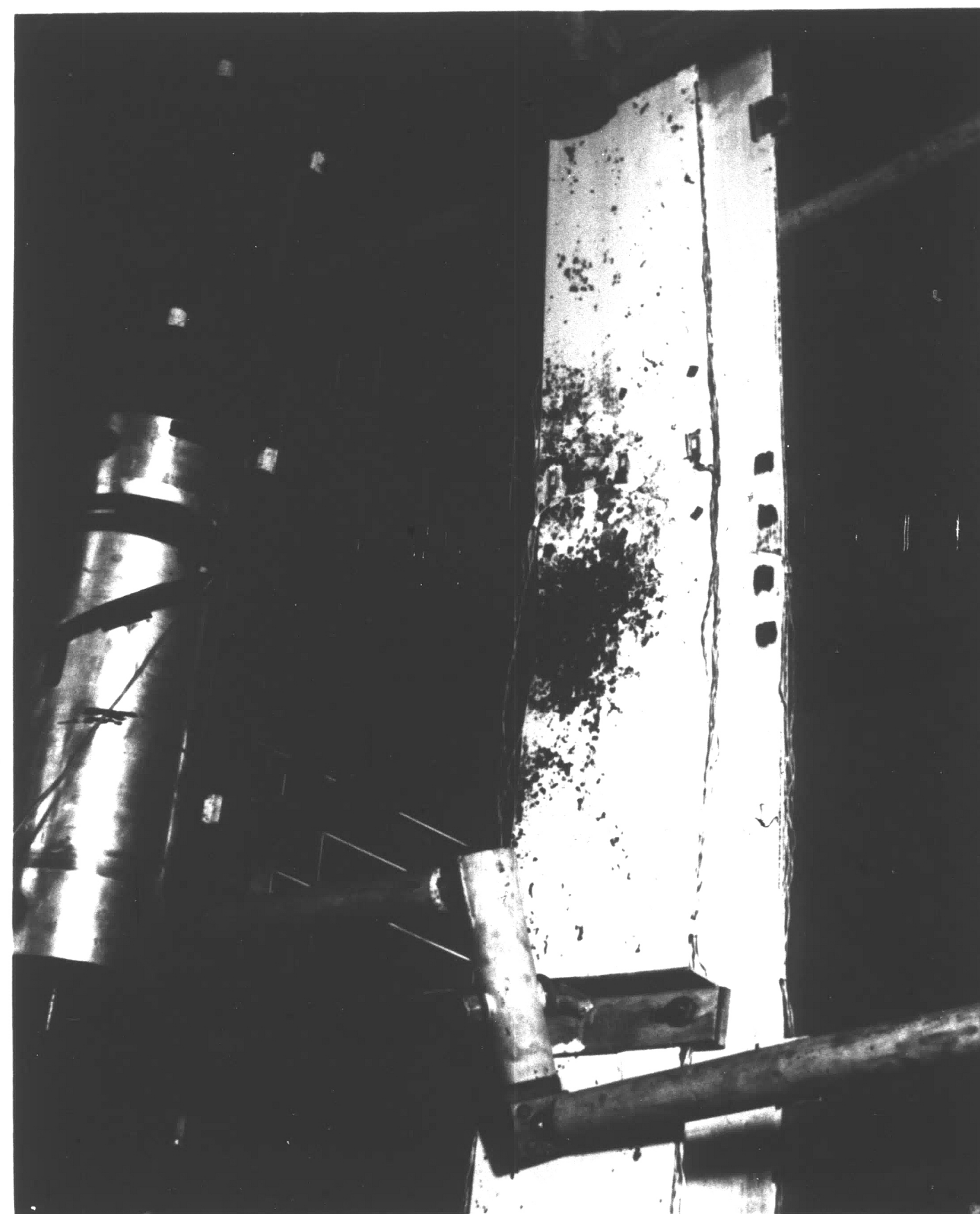
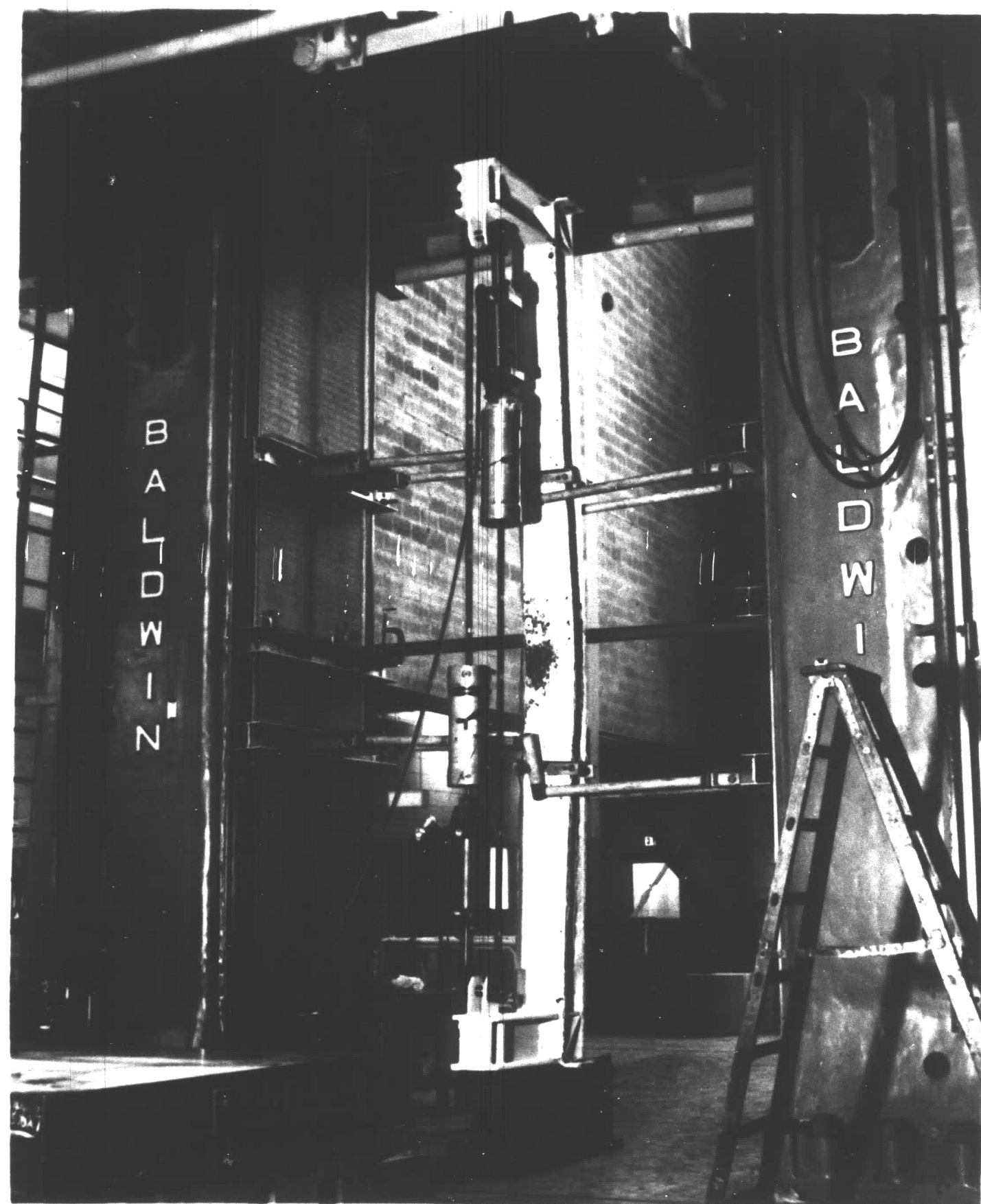


Fig. 21

Failure Mode, 11H66 Beam-Column

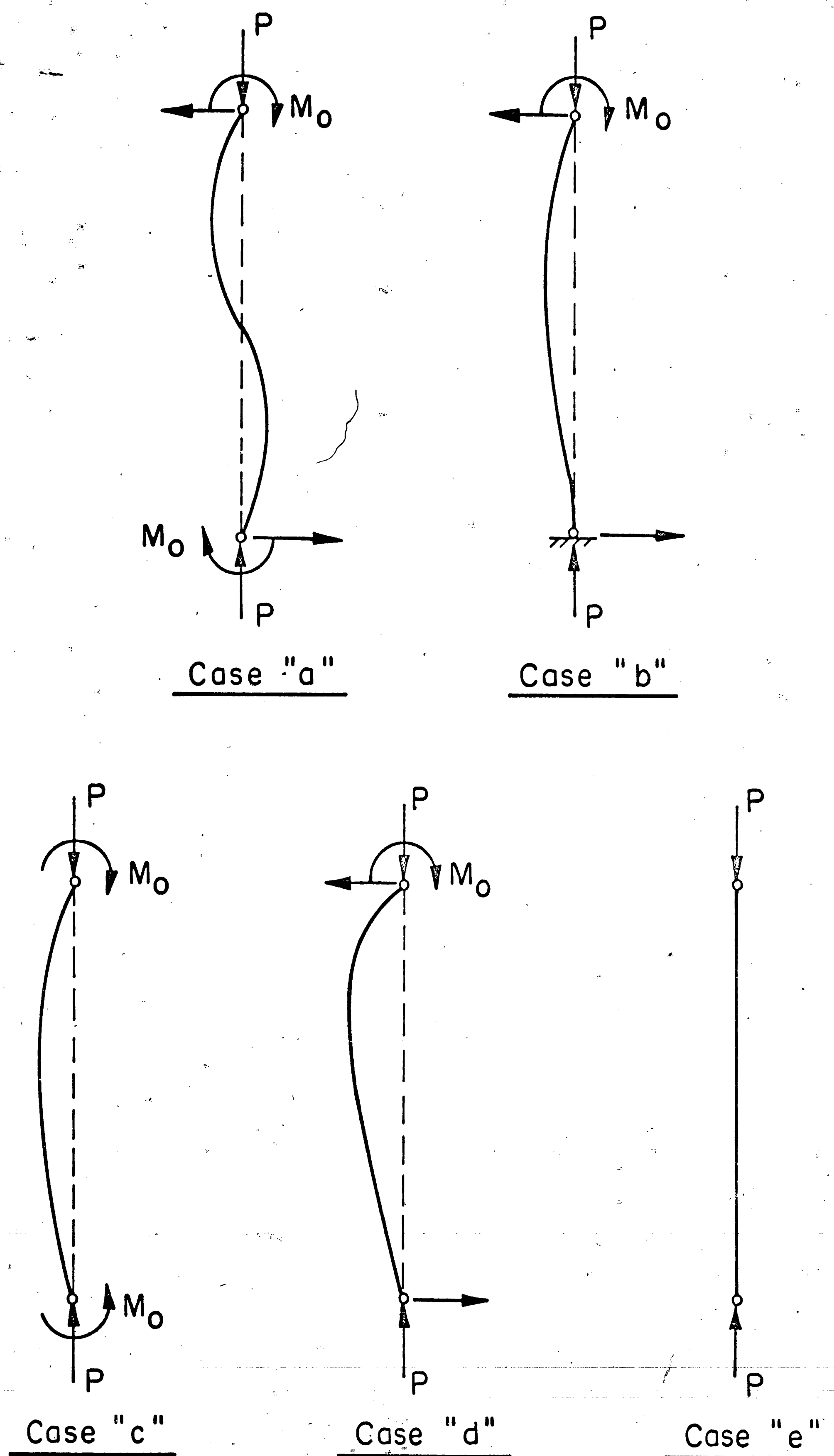


Fig. 22 Loading Conditions for Beam-Columns

INTERACTION CURVE

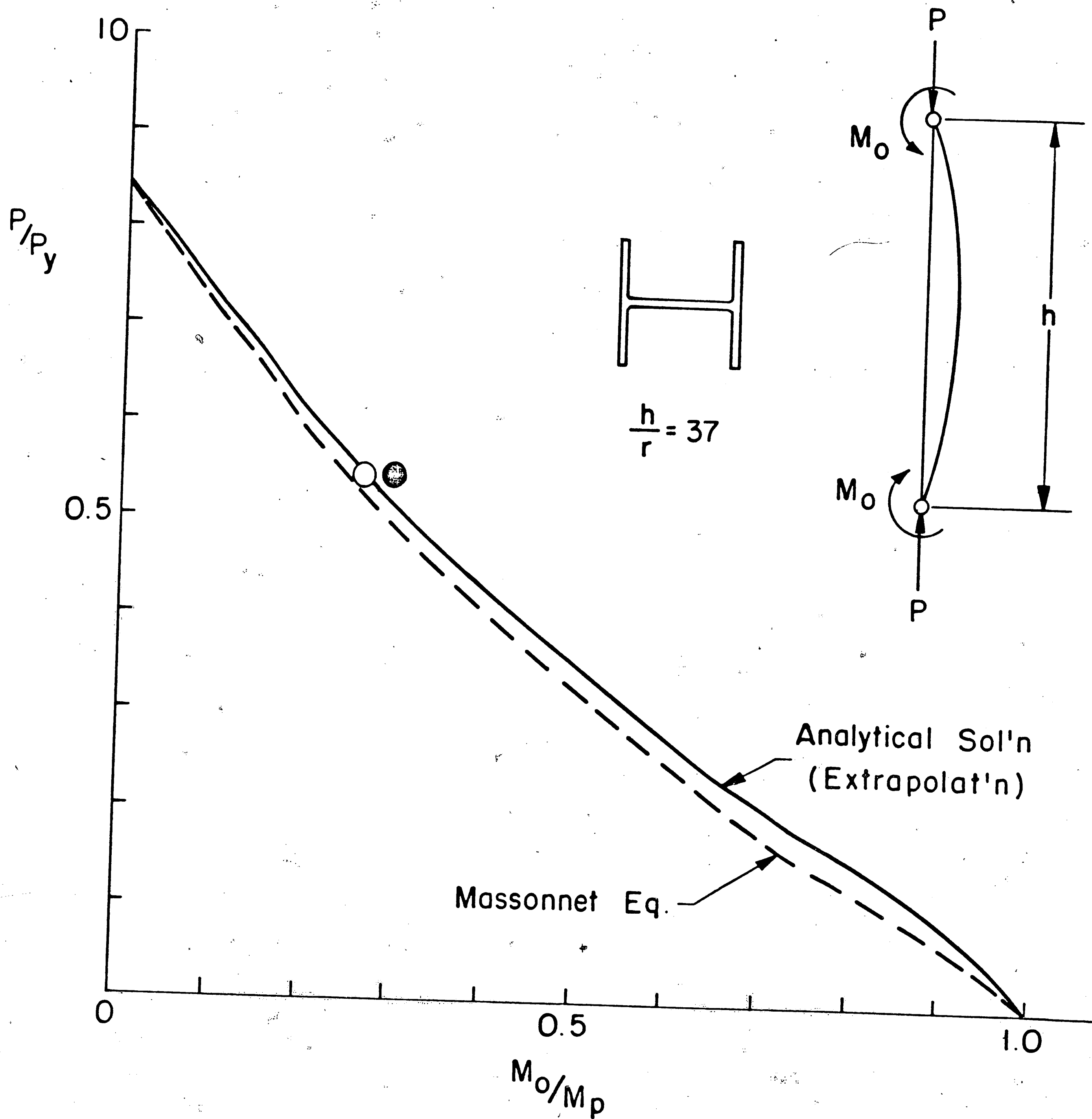


Fig. 23

Test Data and Interaction Curves

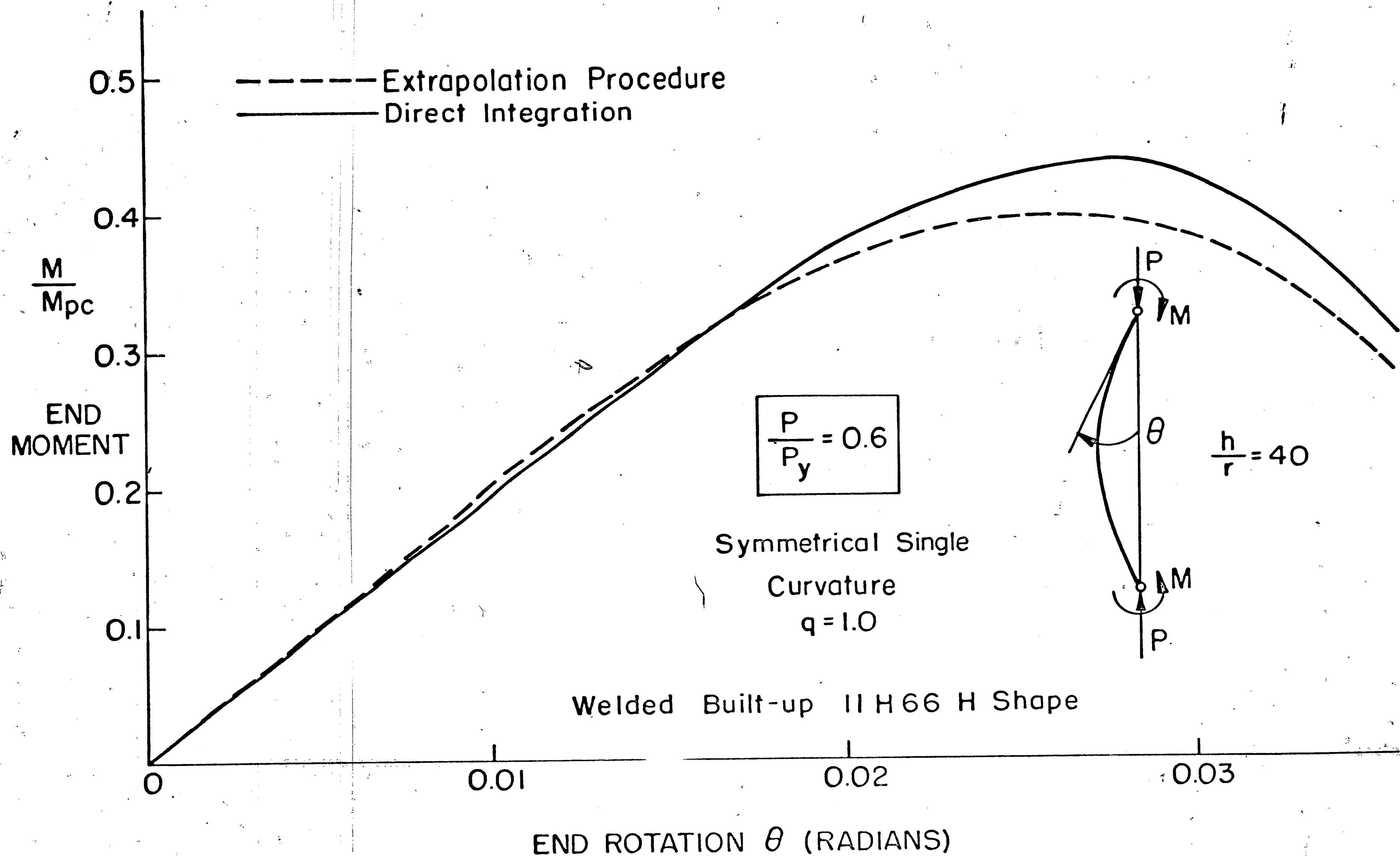
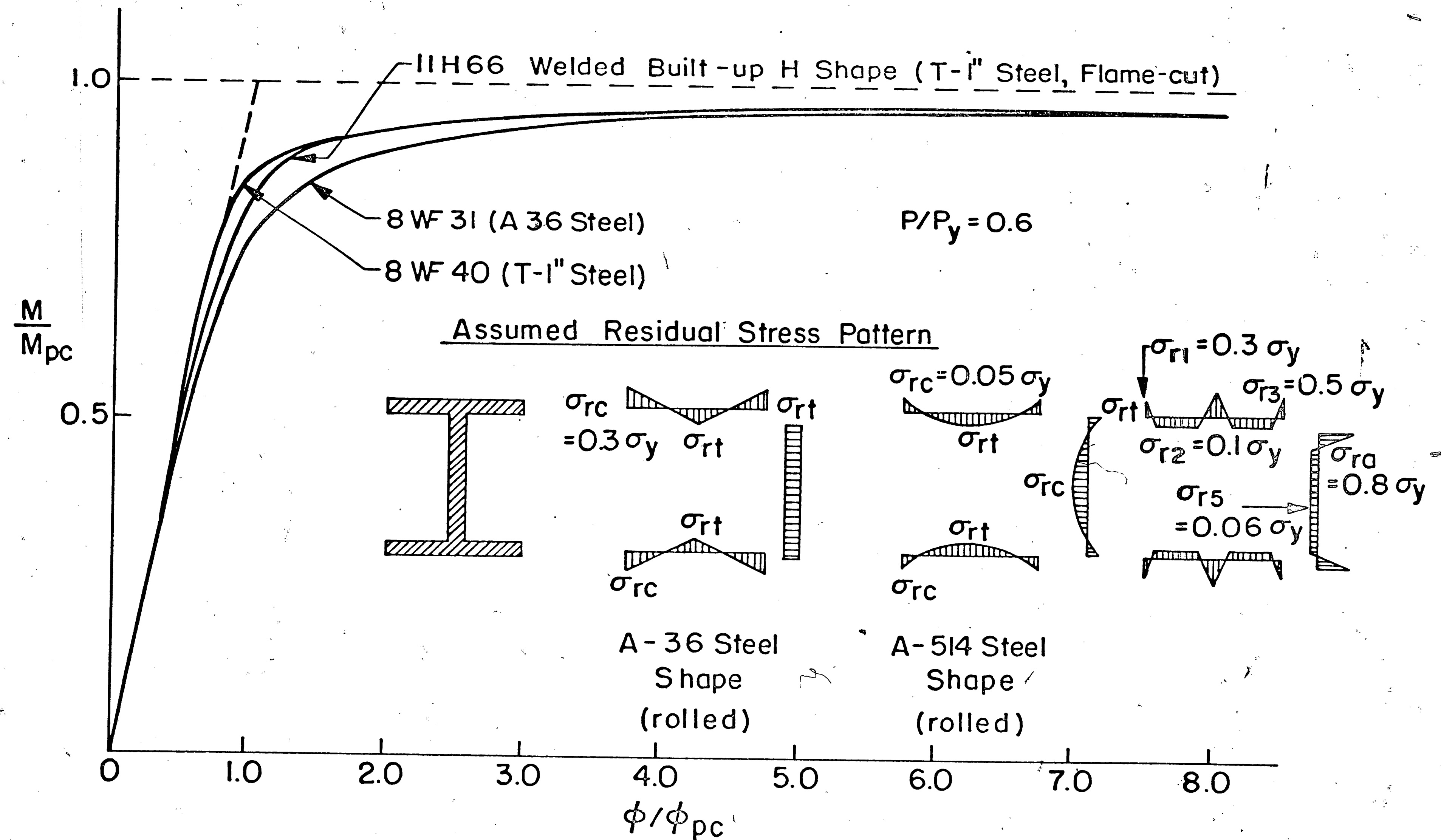


Fig. 24

End-Moment-End Rotation Curve



COMPARISON OF M-P- ϕ CURVES

Fig. 25

Moment-Thrust-Curvature Curves

VI. REFERENCES

1. P. R. Adams
PLASTIC DESIGN IN HIGH STRENGTH STEEL, Ph.D.
Dissertation, Lehigh University, May, 1966
2. U. S. Steel
"T-1" CONSTRUCTIONAL ALLOY STEEL, 2nd Ed.,
June, 1966.
3. A.S.T.M.
STANDARD SPECIFICATION FOR HIGH YIELD STRENGTH
QUENCHED AND TEMPERED ALLOY STEEL PLATE, SUITABLE
FOR WELDING, A.S.T.M., 1964.
4. A.S.T.M.
METHODS AND DEFINITIONS FOR MECHANICAL TESTING
OF STEEL PRODUCTS, A370-65, 1965.
5. N. R. Nagaraja Rao, M. Lohrmann, L. Tall
EFFECT OF STRAIN RATE ON THE YIELD STRESS OF
STRUCTURAL STEEL, A.S.T.M. Journal of Materials,
Vol. 1, No. 1, March, 1966.
6. A. W. Huber, L. S. Beedle
RESIDUAL STRESS AND THE COMPRESSIVE STRENGTH OF
STEEL, Welding Journal, Vol. 33, December, 1954.
7. F. Nishino
BUCKLING STRENGTH OF COLUMNS AND THEIR COMPONENT
PLATES, Ph.D. Dissertation, Lehigh University,
October, 1964.
8. C. K. Yu
INELASTIC COLUMNS WITH RESIDUAL STRESSES, Ph.D.
Dissertation, Lehigh University, (in preparation).
9. B. G. Johnston, Editor
GUIDE TO DESIGN CRITERIA FOR METAL COMPRESSION
MEMBERS, COLUMN RESEARCH COUNCIL, 2nd Ed., Wiley,
1966.
10. L. Tall
STUB COLUMN TEST PROCEDURE, Fritz Laboratory Report
No. 220A.36, February, 1961. Also Document X-282-61,
International Institute of Welding, Oslo, July, 1962.
Also, Appendix B of Ref. 9 ("CRC" Guide).
11. M. G. Lay, R. A. Aglietti, T. V. Galambos
TESTING TECHNIQUES FOR RESTRAINED BEAM-COLUMNS,
Experimental Mechanics, Vol. 6 No. 1, January, 1966.

12. R. C. VanKuren, T. V. Galambos
BEAM-COLUMN EXPERIMENTS, Proc. A.S.C.E., Journal
of the Structural Div. 3876, Vol. 90, No ST2,
April, 1964.
13. E. Yarimci
INCREMENTAL INELASTIC ANALYSIS OF FRAMED STRUCTURES
AND SOME EXPERIMENTAL VERIFICATIONS, Ph.D. Disser-
tation, Lehigh University, May, 1966.
14. A.S.C.E. and W.R.C.
COMMENTARY ON PLASTIC DESIGN IN STEEL, A.S.C.E.
Manual No. 41, 1961.
15. S. P. Timoshenko, J. M. Gere
THEORY OF ELASTIC STABILITY, McGraw-Hill Co.,
New York, 1961.
16. L. W. Lu, et.al.
PLASTIC DESIGN OF MULIT-STORY FRAMES (Lecture Notes),
Fritz Eng. Lab., Lehigh University, August, 1965.
17. L. W. Lu, et.al.
PLASTIC DESIGN OF MULTI-STORY FRAMES (DESIGN AIDS),
Fritz Eng. Lab., Lehigh University, August, 1965.
18. M. Ojalvo, Y. Fukumoto
NOMOGRAPHS FOR THE SOLUTION OF BEAM-COLUMN PROBLEMS,
Welding Research Council Bulletin, No. 78, June, 1962.
19. L. Tall, Editor-in-Chief
STRUCTURAL STEEL DESIGN, Ronald Press, 1964.

VITA

The author was born as the first son of Sakuzo and Chiyo Okuto on September 13, 1937, in Osaka, Japan. He was married to the former Konomi Tashiro in February, 1965. He attended the Osaka University in the Department of Mechanical Engineering from April, 1956 to March, 1960. He received a Bachelor of Engineering Degree in March, 1960.

In April, 1960, he joined the Production Engineering Department, Osaka Steel Works, Sumitomo Metal Industries, Ltd., as a production engineer. Since then he has been studying the welded steel structures.

The author joined the Fritz Engineering Laboratory, Civil Engineering Department, Lehigh University in September, 1965. He has been associated with the research project on Welded and Rolled Heat-Treated "T-1", Columns.